# Revisiting the Anomalous RF Field Penetration Into a Warm Plasma

Igor D. Kaganovich, Oleg V. Polomarov, and Constantine E. Theodosiou

***Abstract*—Radio frequency (RF) waves do not penetrate into a plasma and are damped within it. The electric field of the wave and plasma current are concentrated near the plasma boundary in a skin layer. Electrons can transport the plasma current away from the skin layer due to their thermal motion. As a result, the width of the skin layer increases when electron thermal velocity is taken into account. This phenomenon is called the anomalous skin effect. The anomalous penetration of the RF electromagnetic field occurs not only for the electric field parallel to the plasma boundary (inductively coupled plasmas), but also for the electric field normal to the plasma boundary (capacitively coupled plasmas). Such anomalous penetration of the RF field modifies the structure of the RF sheath in capacitive coupled plasma. Recent advances in the nonlinear, nonlocal theory of the capacitive sheath are reported. It is shown that separating the electric field profile into exponential and nonexponential parts yields an efficient qualitative and quantitative description of the anomalous RF field penetration in both inductively and capacitively coupled plasmas.**

***Index Terms*—Anomalous skin effect, capacitive sheath, radio frequency (RF) discharge, skin layer.**

## I. Introduction

A RADIO frequency (RF) electromagnetic field does not penetrate into a plasma if the field frequency $\omega$ is smaller than the electron plasma frequency $\omega_p = \sqrt{4\pi e^2 n_e/m}$, where $e$ and $m$ are the electron charge and mass, respectively, and $n_e$ is the electron density. Electrons distribute their charge and current so as to shield out the electromagnetic field. The shielding depends on the direction of the electric field with regard to the plasma boundary. If the RF electric field is perpendicular to the plasma boundary, the RF field penetrates into the plasma only within a depth of the order of the Debye length $v_T/\sqrt{2}\omega_p$, where $v_T = \sqrt{2T_e/m}$ is the electron thermal velocity, determined by the electron temperature $T_e$, in electronvolts. If the RF electric field is directed along the plasma boundary, the RF field penetrates into the plasma only within a depth of the order of the skin depth $c/\omega_p$, where $c$ is the speed of light in vacuum. Here, we consider a "collisionless" plasma, i.e., where the collision frequency is small compared to the field frequency $\nu \ll \omega$ and the electrons undergo rare collisions during the RF cycle; thus, collisions have little effect on field screening by the plasma.

Manuscript received June 15, 2005; revised September 30, 2005.This work was supported in part by the U.S. Department of Energy Office of Fusion Energy Sciences through a University Research Support Program and in part by the University of Toledo.

I. D. Kaganovich is with the Plasma Physics Laboratory, Princeton University, Princeton, NJ 08543 USA.

O. V. Polomarov and C. E. Theodosiou are with the Department of Physics and Astronomy, University of Toledo, Toledo, OH 43606-3390 USA.

Digital Object Identifier 10.1109/TPS.2006.873253

Another important scale is the nonlocality or phase-mixing scale $v_T/\omega$, which determines the scale length of spreading of the electron current profile in the plasma. To demonstrate the concept of phase-mixing scale $v_T/\omega$, let us consider a simple model, where an electron acquires a prescribed velocity kick at the plasma boundary, in the direction normal to the boundary

$$dv_x(t) = \Delta V \exp(-i\omega t). \tag{1}$$

The electron velocity at a distance $x$ from the boundary will be determined by the moment when velocity kick was acquired at the plasma boundary, i.e., by the time $t - x/v_x$. The electron current in the plasma is obtained by integrating over contributions of electrons with a velocity distribution function $f(v_x)$

$$j(x,t) = e\Delta V \int_0^\infty f(v_x) \exp[-i\omega(t - x/v_x)]\, dv_x. \tag{2}$$

Here, only electrons collided with the wall ($v_x > 0$) have to be taken into account. For a Maxwellian distribution function $f(v_x) = n_0 e^{-v_x^2/v_T^2}/v_T\sqrt{\pi}$, the plasma current in (2) becomes

$$j(x,t) = \frac{j_0 e^{-i\omega t}}{\sqrt{\pi}} \int_0^\infty \exp\left(-s^2 + \frac{i\omega x}{v_T s}\right) ds \tag{3}$$

where $s = v_x/v_T$ and $j_0 = en_0\Delta V$. The amplitude and phase of the current are shown in Fig. 1. In the limit $\omega x/v_T \gg 1$, the integration in (3) can be performed analytically making use of the method of steepest descent [1] (see Appendix A for more details). This gives

$$j(x,t) \approx \frac{j_0}{\sqrt{3}} \exp\left[-i\omega t - \frac{3}{4}\left(\frac{x}{\lambda_\omega}\right)^{2/3} + i\frac{3\sqrt{3}}{4}\left(\frac{x}{\lambda_\omega}\right)^{2/3}\right] \tag{4}$$

where $\lambda_\omega = v_T/\sqrt{2}\omega$ is the phase-mixing scale. Comparison of the asymptotic calculation result given by (4) with the exact result of numerical integration in (3) is shown in Fig. 1. From Fig. 1, it is evident that (4) approximates the exact result for any $x$ within a 15% error bar. The largest error occurs at $x = 0$, where half of the electron population with velocity $v_x > 0$ acquired the velocity kick, which gives rise to the electron current $j(0) = j_0/2$, whereas (4) predicts $j(0) = j_0/\sqrt{3}$.

Equation (4) describes the process of phase mixing—electrons with velocities different by $\delta v_x \sim v_T$ have different phase lag of the order $\omega x/v_T$ at a distance $x$ from the plasma boundary. Therefore, at $x \sim v_T/\omega$, the phase difference becomes considerable: contributions to the total current from electrons with different velocities $v_x$ cancel out each other, and the plasma current vanishes. Interestingly, the spatial profile

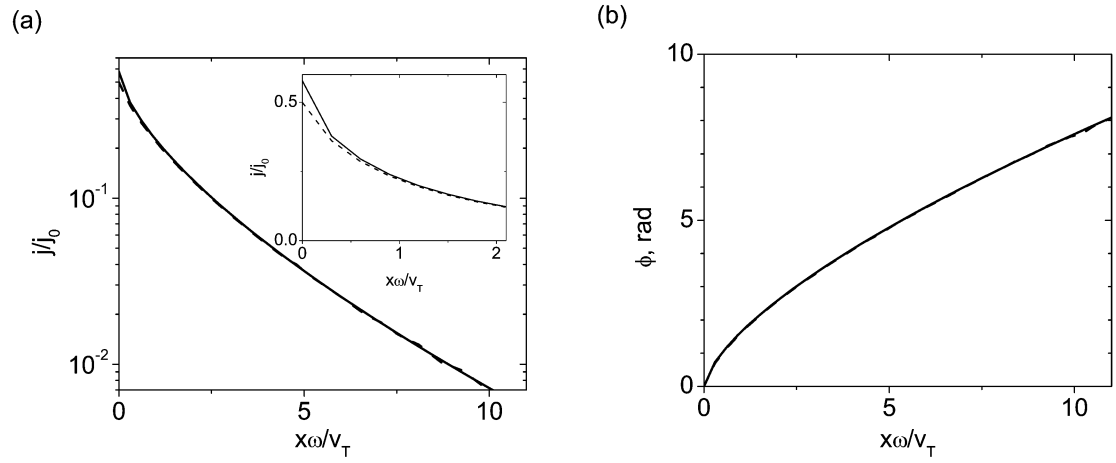


Fig. 1. Phase-mixing of the test particle current generated by velocity kicks $\Delta V\cos(\omega t)$ at the plasma boundary: (a) current amplitude and (b) the current phase with respect to the phase of the velocity kick at the plasma boundary. Amplitude of the current is normalized on $j_0 = en_0\Delta V$, where $n_0$ is plasma density. Solid lines show the exact result of numerical integration in (3), dashed lines show the asymptotic, approximate analytical results given by (4).

of the current is not a simple exponential function, but an exponential function of $(x/\lambda_\omega)^{2/3}$. As will be shown below this is typical for the spatial profiles of the electric field and electron current in warm plasmas due to nonlocal effects.

So far, we solved only test particle problem and did not take into account the plasma polarization. The current in (3) is nonuniform; thus, there must be an electron density perturbation according to the continuity equation

$$e\frac{\partial n_e}{\partial t} = -\frac{\partial j}{\partial x}. \tag{5}$$

The electron density perturbations polarize the plasma and generate an electric field, which in turn, affects the electron motion and the electron current profile. Thus, (3) has to be modified to include the self-consistent electric field. This requires solving the Vlasov equation together with the Poisson equation. In his famous 1946 paper, Landau obtained an analytic solution for the penetration of the longitudinal RF electric field into a plasma [2]. Note that he also described "Landau damping" in the same paper. We briefly review his solution for a small amplitude electric field in the linear approximation and discuss the more realistic case of a large amplitude electric field.

The structure of this review is as follows. In Section II, the penetration of the longitudinal electric field into the plasma is described. This case corresponds to the RF sheath in a capacitively coupled plasma. In Section III, the penetration of the transverse electric field into the plasma is studied, which corresponds to an inductively coupled plasma. In Section III-E, it is shown that anisotropy of the electron velocity distribution function can have a profound effect on the anomalous skin effect.

## II. Penetration of the RF Electric Field Directed Perpendicular to the Plasma Boundary (Capacitively-Coupled Plasma)

### A. Small-Amplitude Electric Field

In the previous section, we considered a test particle current driven by artificially applied velocity modulations at the plasma boundary. Here, self-consistent penetration of a small amplitude RF electric field directed perpendicular to the plasma boundary is considered. Such a model provides some insight into the sheath structure of capacitively coupled plasmas.

First, let us consider a stationary negatively biased electrode. It is well known that the externally applied electric field penetrates inside the plasma over distances of the order of the Debye length $a = v_T/\sqrt{2}\omega_p = \sqrt{T_e/4\pi e^2 n_0}$. The plasma electrons are trapped by the plasma potential, $\phi(x)$, in the potential well $-e\phi(x)$. The electron density obeys the Boltzmann distribution

$$n_e(x) = n_0\exp[e\phi(x)/T_e]. \tag{6}$$

The Poisson equation

$$\frac{d^2\phi}{dx^2} = -4\pi e(n_i - n_e) \tag{7}$$

can be simplified assuming small potential variations $-e\phi(x)/T_e \ll 1$ and a uniform background plasma with $n_e = n_i = n_0$. Thus, (7) becomes

$$\frac{d^2\phi}{dx^2} = \frac{4\pi e^2 n_0}{T_e}\phi. \tag{8}$$

The solution of (8) is an exponentially decaying electric field $E = -d\phi/dx$

$$E = E_0\exp\left(-\frac{x}{a}\right). \tag{9}$$

Here, $E_0$ is the value of the electric field at the plasma boundary. This is the solution for a static, time-independent sheath electric field. In the opposite case of the time-dependent electric field, the electrons are no longer in static equilibrium with the electric field and Boltzmann distribution given by (6) is not valid, therefore, the electron density has to be determined from the Vlasov equation. Landau solved the Vlasov equation coupled

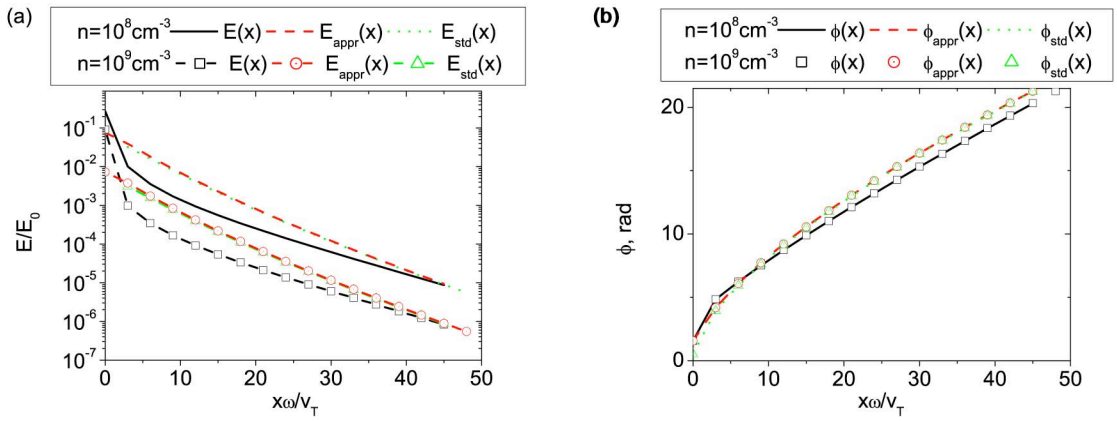


Fig. 2. Penetration of the external electric field into a plasma. Only part of the electric field $E_t(x)$ is shown (color online). Solid (black) lines show the exact solution given by (11); dashed (red) lines and subscript appr correspond to the approximate calculation of (14); dotted (green) lines and the subscript std correspond to the approximate calculation in the limit $x \gg \lambda_\omega$ obtained making use the method of the steepest descend given by (15). RF electric field frequency is 13.56 MHz and the plasma density is $10^8$ cm$^{-3}$ (lines) and $10^9$ cm$^{-3}$ (symbols).

with the Poisson equation analytically in the linear approximation considering an electrostatic field with small amplitude $|e\phi(x)|/T_e \ll 1$ and small frequency $\omega \ll \omega_p$ [2]. Details of the solution are described in Appendix B.

To summarize, the solution can be separated into three parts

$$E_x(x,t) = \left[E_0 \exp\left(-\frac{x}{a}\right) + E_b + E_t(x)\right] e^{-i\omega t}. \quad (10)$$

Here, $E_0$ is the amplitude of the electric field at the plasma boundary, $E_b = E_0/\varepsilon$ is the electric field in the plasma bulk far away from the sheath region, $\varepsilon = 1 - \omega_p^2/\omega^2$ is the dielectric constant of the cold plasma, and $E_t(x)$ is the electric field in a transient region with a spatial length of order $v_T/\omega$. The first term is the Debye screening of the external electric field. The second part describes a small, uniform electric field penetrating into the plasma far away from the boundary. The second and third terms are absent for a time-independent, static applied electric field and appear only in the case of the RF electric field. The solution for the transient electric field $E_t(x)$ profile is derived in Appendix B and is given by

$$E_t(x) = \frac{2E_0}{\pi} \int_0^\infty \frac{1}{k} \frac{\mathrm{Im}[\varepsilon_{||}(\omega,k)]}{\varepsilon_{||}^*(\omega,k)\varepsilon_{||}(\omega,k)} e^{ikx}\, dk \quad (11)$$

where $\varepsilon_{||}(\omega,k)$ is the longitudinal plasma permittivity ($\mathbf{E} \,||\, \mathbf{k}$)

$$\varepsilon_{||}(\omega,k) \simeq 1 + \frac{2\omega_p^2}{k^2 v_T^2}\left[1 + \frac{\omega}{kV_T} Z\left(\frac{\omega}{kV_T}\right)\right] \quad (12)$$

and $Z(\zeta)$ is the plasma dispersion function [4]

$$Z(\xi) = \pi^{-1/2} \int_{-\infty}^{\infty} dt \frac{\exp(-t^2)}{t-\xi}, \quad \mathrm{Im}\xi > 0. \quad (13)$$

In the limit $x \gg \lambda_\omega$, only small $k$ contribute to the integral and $\varepsilon_{||}(\omega,k)$ can be substituted by $\varepsilon_{||}^*(\omega,0) \equiv \varepsilon$ in the denominator of (14), which gives

$$E_t(x) \approx E_{\mathrm{appr}}(x) = \frac{2E_0}{\pi\varepsilon^2} \int_0^\infty \frac{1}{k} \mathrm{Im}[\varepsilon_{||}(\omega,k)] e^{ikx}\, dk. \quad (14)$$

Application of the method of steepest descent to (14) yields [2]

$$E_t(x) \approx E_{\mathrm{std}}(x) = \frac{2E_0}{\sqrt{3}\varepsilon^2} \frac{\omega_p^2}{\omega^2} \left(\frac{x}{\lambda_\omega}\right)^{2/3} \times \exp\left[\left(-\frac{3}{4} + i\frac{3\sqrt{3}}{4}\right)\left(\frac{x}{\lambda_\omega}\right)^{2/3} - i\pi/3\right] \quad (15)$$

where $\lambda_\omega = v_T/\sqrt{2}\omega$ is the phase-mixing scale. The plots of the amplitude and phase of the electric field profile $E_t(x)$ given by (11) and the approximate $E_{\mathrm{appr}}(x)$ given by (14), and asymptotic analytical result $E_{\mathrm{std}}(x)$ given by (15) are shown in Fig. 2. Fig. 2 shows that the steepest descent method given by (15) closely approximates (14) already for $x > v_T/\omega$. However, the both asymptotic solutions in (14) and (15) approximate the full solution in (11) only for very large $x > 40v_T/\omega$. This is due to substituting $\varepsilon(\omega,k)$ by $\varepsilon(\omega,0)$, which results in a considerable error for $k \sim \omega/v_T$ or $x \sim v_T/\omega$.

It follows from (15) that the electric field amplitude at $x > v_T/\omega$ is of order $E_0/\varepsilon$, i.e., it is comparable with the electric field far away from the boundary ($E_t \sim E_b$).

The origin of the electric field $E_t(x)$ can be explained by analyzing the individual electron dynamics. After passing through the region of the RF field, an electron acquires changes $\Delta\varepsilon(v_x)$ in energy and $\Delta u(v_x)$ in velocity

$$\Delta\varepsilon(v_x) = \int_{-\infty}^{\infty} v_x e E[x(t),t] dt$$
$$\Delta u(v_x) = \frac{\Delta\varepsilon}{m v_x}. \quad (16)$$

Here, the electron trajectory is $x(t) = v_x t$, $v_x = |v_x|\mathrm{sgn}(t)$, and the electric field profile is given by (10). The total velocity kick is the summation over velocity kicks due to exponential, bulk and transitional electric fields

$$\Delta u(v_x) = \Delta u_0 + \Delta u_b + \Delta u_t. \quad (17)$$

Substituting an exponential electric field into (16) gives the corresponding electron velocity kick

$$\Delta u_0(v_x) \simeq \frac{2eE_0}{m\omega}\frac{\omega^2 a^2}{v_x^2+(\omega a)^2}. \tag{18}$$

Substituting the uniform electric field $E_b$ into (16) gives the electron velocity

$$\Delta u_b(v_x) \simeq \frac{2eE_0}{im\omega\varepsilon}. \tag{19}$$

This calculation can also be explained as follows. An electron has the oscillating velocity $\Delta u_s = eE_b i/m\omega$ in a uniform RF electric field and a thermal velocity $v_x$. After a collision with the wall, an electron changes its velocity direction. If the initial average velocity was $v_x < 0$, after the collision with the wall with specular reflection, the new average velocity $v_x' > 0$ will change according to

$$v_x' + \Delta u_s(t) = -[v_x + \Delta u_s(t)] \tag{20}$$

or the average velocity changes to

$$v_x' = -v_x - 2\Delta u_s(t) \tag{21}$$

which results in the effective velocity kick of (19).

The origin of the electric field in the transition region $E_t(x)$ is due to the plasma polarization. The velocity perturbations $\Delta u_s(v_x,t)$ produce bunches in the electron density, which, in turn, generate the electric field $E_t(x)$. The decay of the electric field $E_t(x)$ is due to phase mixing similarly to the test-particle case in (4). Thus, generation of the transitional electric field $E_t(x)$ can be considered as a plasma self-consistency effect.

The electric field $E_t(x)$ generates a significant portion of the total velocity kick and thus noticeably influences the electron heating in the RF electric field. Fig. 3 shows the amplitude of the electron velocity kick $\Delta u(v_x)$ due to the interaction with the electric field given by (10). Electrons with small velocities $v_x \sim \omega a = v_T\omega/\omega_p$ pick up a large velocity kick due to the exponential electric field $E_0\exp(-x/a - i\omega t)$, $\Delta u \simeq \Delta u_0 \sim 2eE_0/m\omega$. For very large electron velocities $v_x \gg v_T$, the velocity kick given by (18) becomes small and the main contribution to the velocity kick comes from the uniform electric field $E_b = E_0 e^{-i\omega t}/\varepsilon$ and the collision with the wall, $\Delta u \simeq \Delta u_b \sim 2eE_0/m\omega\varepsilon$. In the intermediate range of velocities $v_x \sim v_T$, the account of the electric field $E_t(x)$ is important, as in this case $\Delta u_t \sim \Delta u_b$. As is evident from Fig. 3, taking this electric field $E_t(x)$ into account results in a considerable reduction of the electron velocity kick $v_x \sim v_T$ for the bulk of the electron population compared with the case when this electric field is not taken into account. Note that most models neglect the electric field $E_t(x)$, see, for example [7] and [8].

### B. Large Amplitude Electric Field

In many practical applications of capacitively coupled plasmas, the value of the external electric field is large: the potential drop in the sheath region $V_{\rm sh}$ is typically of the order of hundreds of volts and is much larger than the electron temperature $T_e$, which is of the order of a few volts; consequently, the electric field penetration has to be treated nonlinearly.

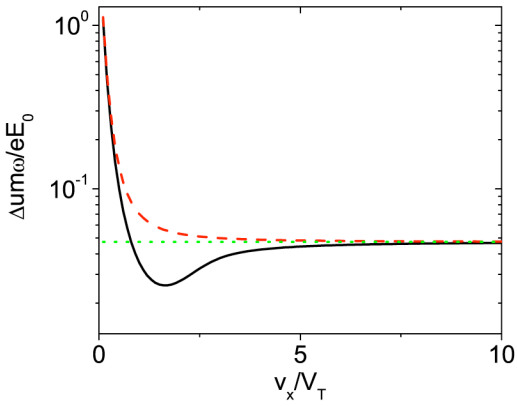


Fig. 3. Electron velocity kick after interaction with the RF electric field. Solid line shows a velocity kick $\Delta u$ calculated according to the full electric field in (10). Dashed line shows a $\Delta u$ due to the electric field $E_0\exp(-x/a)$ and the uniform electric field $E_b$ only; the dotted line is due to $E_b$. RF electric field frequency is 13.56 MHz and the plasma density is $10^8$ cm$^{-3}$.

In the limit $V_{\rm sh} \gg T_e$, a wall is charged negatively all time with an alternating charge in a manner to conduct an ac current, driven by an external electric circuit. A negative charge pushes electrons away from the electrode up to a distance where its electric field is screened by a positive ion density. As $V_{\rm sh} \gg T_e$, the sheath width is much larger than the Debye length, and the plasma sheath boundary can be considered as infinitely thin. The position of the boundary is determined by the condition that the external electric field is screened in the sheath regions when and where electrons are absent [5]–[7], [9].

Electron interactions with the sheath electric field are traditionally treated as collisions with a moving potential barrier (wall). It is well known that multiple electron collisions with an oscillating wall result in electron heating, provided there is sufficient phase-space randomization in the plasma bulk. It is common to describe the sheath heating by considering electrons as test particles, and neglecting the plasma electric field [8]. As was pointed out in [7], [10], [11], and [52] accounting for the electric field in the plasma reduces the electron sheath heating, and the electron sheath heating vanishes completely in the limit of uniform plasma density. Therefore, an accurate description of the RF fields in the bulk of the plasma is necessary for calculating the sheath heating. The electron velocity is oscillatory in the sheath, and as a result of these velocity modulations, the electron density bunches appear in the region adjacent to the sheath, similar to the previously described case of small-amplitude field, see Fig. 4. These electron density perturbations decay due to phase mixing over a length of order $v_T/\omega$, where $v_T$ is the electron thermal velocity, and $\omega$ is the frequency of the electric field. The electron density perturbations polarize the plasma and produce an electric field in the plasma bulk. This electric field, in turn, changes the velocity modulations and correspondingly influences the electron density perturbations. Therefore, electron sheath heating has to be studied in a self-consistent nonlocal manner assuming a finite-temperature plasma.

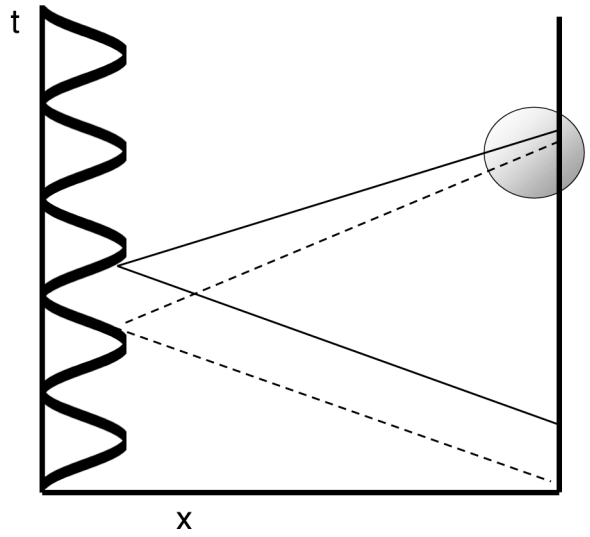


Fig. 4. Schematic of density bunches formation in the region adjacent to the sheath. Plasma-sheath boundary is shown by bold solid line. Electrons with the same velocity $v_x$ and distance apart $\sim v_x/\omega$ collide with the sheath. First electron looses its energy and decelerates, whereas the second acquire energy and accelerates. As a result, the distance between two electrons decreases, which produces electron density perturbations.

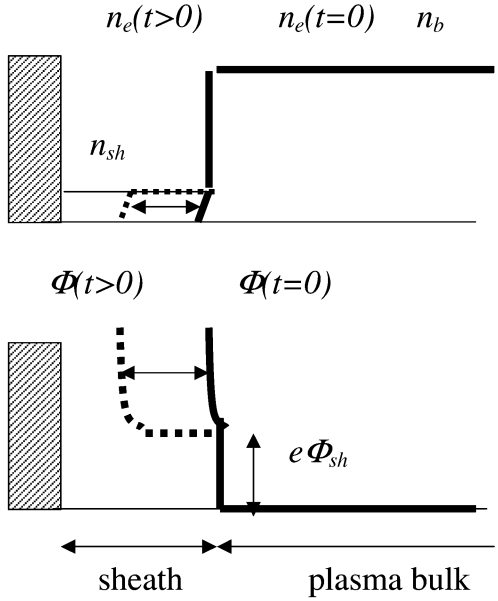


Fig. 5. Schematic of a sheath. Negatively charged electrode pushes electrons away at different distances depending on the strength of the electric field at the electrode. Shown are the density and potential profiles at two different times. Solid line is at the time of maximum sheath expansion.

Notwithstanding the fact that particle-in-cell (PIC) simulations results have been widely available for the past decade [12], [13], a basic understanding of the electron heating by the sheath electric field is incomplete, because no one has studied the electric field in the plasma bulk using a kinetic approach, similar to the anomalous skin effect for the inductive electric field [3]. In this regard, analytical models are of great importance because they shed light on the most complicated features of collisionless electron interactions with the sheath. In [14], an analytical model was developed to explore the effects associated with the self-consistent nonlocal nature of this phenomenon.

One of the approaches to study electron sheath heating is based on a fluid description of the electron dynamics. For the collisionless case, closure assumptions for the viscosity and heat fluxes are necessary. In most cases, the closure assumptions are made empirically or phenomenologically [13], [15]. The closure assumptions have to be justified by direct comparison with the results of kinetic calculations as is done, for example, in [16] and [17]. Otherwise, inaccurate closure assumptions may lead to misleading results as discussed below. Traditional assumptions have been made for discharge parameters [5]–[7], [9], as follows. The discharge frequency is assumed to be small compared with the electron plasma frequency. Therefore, most of the external electric field is screened in the sheath region by an ion space charge. The ion response time is typically larger than the inverse discharge frequency, and the ion density profile is quasi-stationary. There is an ion flow from the plasma bulk towards the electrodes. In the sheath region, ions are being accelerated towards the electrode by the large sheath electric field, and the ion density in the sheath region is small compared with the bulk ion density.

To model the sheath-plasma interaction analytically, the additional simplifying assumptions of two-step ion density profile have been adopted [14], [20]. In the present analytical treatment, the ion density profile is assumed fixed and is modelled in a two-step approximation: the ion density $n_b$ is uniform in the plasma bulk, and the ion density in the sheath $n_{\rm sh} < n_b$ is also uniform (see Fig. 5). At the sheath-plasma boundary, there is a stationary potential barrier for the electrons $(e\Phi_{\rm sh})$, so that only the energetic electrons reach the sheath region. The potential barrier is determined by the quasi-neutrality condition, i.e., when the energetic electrons enter the sheath region, their instantaneous density is equal to the ion density $[n_e(\Phi_{\rm sh}) = n_{\rm sh}]$

The electron density profile is time-dependent in response to the time-varying sheath electric field. The large sheath electric field does not penetrate into the plasma bulk. Therefore, the quasi-neutrality condition holds in the plasma bulk, i.e., the electron density is equal to ion density, $n_e = n_b$. In the sheath region, the electrons are reflected by the large sheath electric field. Therefore, $n_e = n_{\rm sh}$ for $x > x_{\rm sh}(t)$ , and $n_e = 0$ for $x < x_{\rm sh}(t)$, where $x_{\rm sh}(t)$ is the position of the plasma-sheath boundary [5]–[7], [9]. From Maxwell's equations, it follows that $\nabla \cdot \mathbf{J} = 0$, where the total current $\mathbf{J}$ is the sum of the displacement current and the electron current. In the one-dimensional (1-D) case, the condition $\nabla \cdot \mathbf{J} = 0$ yields the conservation of the total current [2], [9]

$$en_eV_e + \frac{1}{4\pi}\frac{\partial E_{\rm sh}}{\partial t} = j_0 \sin(\omega t + \phi) \tag{22}$$

where $j_0$ is the amplitude of the RF current controlled by an external circuit and $\phi$ is the initial phase. In the sheath, electrons are absent in the region of large electric field, and (22) can be integrated to give [9]

$$E_{\rm sh}(x,t) = \frac{4\pi j_0}{\omega}[-1 - \cos(\omega t + \phi)] + 4\pi|e|n_{\rm sh}x, \quad x < x_{\rm sh}(t) \tag{23}$$

where Poisson's equation has been used to determined the spatial dependence of the sheath electric field. The first term on the right-hand side of (23) describes the electric field at the electrode and the second term relates to the ion space charge screening of the sheath electric field. The position of the plasma-sheath boundary $x_{\rm sh}(t)$ is determined by the zero of the sheath electric field, $E_{\rm sh}[x_{\rm sh}(t),t]=0$. From (23), it follows that

$$x_{\rm sh}(t)=\frac{V_{\rm sh0}}{\omega}[1+\cos(\omega t+\phi)] \tag{24}$$

where $V_{\rm sh0}=j_0/(en_{\rm sh})$ is the amplitude of the plasma-sheath boundary velocity. The ion flux on the electrode is small compared with the electron thermal flux. Because electrons attach to the electrode, the electrode surface charges negatively, so that in a steady-state discharge, the electric field at the electrode is always negative, preventing an electron flux on the electrode. However, for a very short time (in the vicinity of $\omega t_n+\phi\approx\pi(1+2n)$), the sheath electric field vanishes, allowing electrons to flow to the electrode for compensation of the ion flux. Note that there is a large difference between the sheath structure in the discharge and the sheath for obliquely incident waves interacting with a plasma slab without any bounding walls. Because electrodes are absent, electrons can move outside the plasma, and the electric field in the vacuum region, $E_{\rm sh}(x,t)=(4\pi j_0/\omega)\cos(\omega t+\phi)$, may have an alternating sign. Therefore, electrons may penetrate into the region of large electric field during the time when $E_{\rm sh}(x,t)>0$ [18], [19]. In the discharge, however, because the sheath electric field given by (23) always reflects electrons, the electrons *never* enter the region of the large sheath electric field, which is opposite to the case of obliquely incident waves.

I) Collisionless Heating in Capacitive Sheath Making Use of the Two-Step Ion Density Profile Model: The calculations based on the two-step ion density profile model are known to yield discharge characteristics in good agreement with experimental data and full-scale simulations [20].

For analytical calculation of the RF electric field inside the plasma, a linear approximation is used for the plasma conductivity. The validity of the linear approximation is based on the fact that the plasma-sheath boundary velocity and the mean electron flow velocity are small compared with the electron thermal velocity, $V_{\rm sh}\ll v_T$, [9], [12]. The important spatial scale is the length scale for phase mixing, $\lambda_\omega$. The sheath width satisfies $2V_{\rm sh0}/\omega\ll\lambda_\omega$ because $V_{\rm sh}\ll v_T$. Therefore, the sheath width is neglected, and electron interactions with the sheath electric field are treated as a boundary condition. The collision frequency ($\nu$) is assumed to be small compared with the discharge frequency ($\nu\ll\omega$), and correspondingly the mean free path is much larger than the length scale for phase mixing. Therefore, the electron dynamics is assumed to be collisionless. The discharge gap is considered to be sufficiently large compared with the electron mean free path, so that the influence of the opposite sheath is neglected. The effects of a finite gap width leading to bounce resonances have been discussed in [21] and [22].

The electron interaction with the large electric field in the sheath is modelled as a collision with a moving oscillating rigid barrier with velocity $V_{\rm sh}(t)=dx_{\rm sh}(t)/dt$ [5]. After a collision with the plasma-sheath boundary—modelled as a rigid barrier moving with velocity $V_{\rm sh}(t)$—an electron with initial velocity $-u$ acquires a velocity $u+2V_{\rm sh}$. Therefore, the power deposition density transfer from the oscillating plasma-sheath boundary is given by [5], [7]

$$P_{\rm sh}=\frac{m}{2}\left\langle\int_{-V_{\rm sh}}^{\infty}du[u+V_{\rm sh}(t)]\times[(2V_{\rm sh}(t)+u)^2-u^2]f_{\rm sh}(-u,t)\right\rangle \tag{25}$$

where $m$ is the electron mass, $f_{\rm sh}(-u,t)$ is the electron velocity distribution function in the sheath, and $\langle\cdots\rangle$ denotes a time average over the discharge period. Introducing a new velocity distribution function $g(-u_1,t)=f_{\rm sh}[-u-V_{\rm sh}(t),t]$, (25) yields [5], [7]

$$P_{\rm sh}=-2m\left\langle V_{\rm sh}(t)\int_0^{\infty}u_1^2g(-u_1,t)\,du_1\right\rangle \tag{26}$$

where $-u_1=-u-V_{\rm sh}$ is the electron velocity relative to the oscillating rigid barrier. From (26) it follows that, if the function $g(u_1)$ is stationary, then ($P_{\rm sh}=0$) and there is no collisionless power deposition due to electron interaction with the sheath [7], [15], [23]. For example, in the limit of a uniform ion density profile $n_{\rm sh}=n_b$, $g(u_1)$ is stationary (*in an oscillating reference frame of the plasma-sheath boundary*), and the electron heating vanishes [7], [9]. Indeed, in the plasma bulk, the displacement current is small compared with the electron current, and from (22) it follows that the electron mean flow velocity in the plasma bulk

$$V_b(t)=-\frac{j_0}{en_b}\sin(\omega t+\phi) \tag{27}$$

is equal to the plasma-sheath velocity $V_{\rm sh}(t)$, from (24). *Therefore, the electron motion in the plasma is strongly correlated with the plasma-sheath boundary motion*. From the electron momentum equation it follows that there is an electric field, $E_b=m/e\,dV_b(t)/dt$, in the plasma bulk. In a frame of reference moving with the electron mean flow velocity, the sheath barrier is stationary, and there is no force acting on the electrons, because the electric field is compensated by the inertial force ($eE_b-mdV_b(t)/dt=0$). Therefore, electron interaction with the sheath electric field is totally compensated by the influence of the bulk electric field, and the collisionless heating vanishes [10]. The example of a uniform density profile shows the importance of a self-consistent treatment of the collisionless heating in the plasma. If the function $g(u_1,t)$ is nonstationary, there is net power deposition. In [14], a kinetic calculation is performed to yield the correct electron velocity distribution function $g(u_1,t)$ and, correspondingly, the net power deposition.

The electron motion is different for low-energy electrons with an initial velocity in the plasma bulk $|u|<u_{\rm sh}$, where

$$u_{\rm sh}^2=2e\Phi_{\rm sh}/m \tag{28}$$

and for energetic electrons with velocity $|u| > u_{\rm sh}$. The low energy electrons with initial velocity $-u$ in the plasma bulk are reflected from the stationary potential barrier $e\Phi_{\rm sh} = T_e \ln(n_b/n_{\rm sh})$, and then return to the plasma bulk with velocity $u$. High energy electrons enter the sheath region with velocity

$$u' = -\left(u^2 - u_{\rm sh}^2\right)^{1/2}. \tag{29}$$

They acquire a velocity $u'' = 2V_{\rm sh} - u'$ after collision with the moving rigid barrier, and then return to the plasma bulk with a velocity $(u''^2 + u_{\rm sh}^2)^{1/2}$ [24].

As the electron velocity is modulated in time during reflections from the plasma-sheath boundary, so is the energetic electron density (by continuity of the electron flux). This phenomenon is identical to the mechanism of klystron operation [25]. The perturbations in the energetic electron density yield an electric field in the transition region adjusted to the sheath, see Fig. 4.

The solution for the electric field $E_t(x)$ was obtained analytically in [14]. Similar to the previous section, the solution is an expression for the inverse Fourier transform. It cannot be represented in an analytical form and has to be simulated numerically. This simulation has been performed for $n_{\rm sh}/n_b = 1/3$, $\omega/\omega_p = 1/100$, and a Maxwellian electron distribution function. The electric field profile is close to $E_t(x) \approx E_{t0}\exp(-x/\lambda_c)$, where $E_{t0} = -0.72T_e/\lambda_\omega$, and $\lambda_c = (0.19 + 0.77i)\lambda_\omega$ for $x < 6V_T/\omega$. For $x > 6V_T/\omega$, the electric field profile is no longer a simple exponential function, which is similar to the case considered in the previous section.

The difference in phase of the currents of the energetic and low-energy electrons was observed in [13], but it was misinterpreted as the generation of electron acoustic waves. Electron acoustic waves are similar to the ion sound waves where cold electron population play role of ions. Electron acoustic waves can be excited if there is a complex value of $k$, which is the root of the plasma dielectric function $\varepsilon(\omega, k) = 0$ for a given $\omega$, with small damping $\mathrm{Im}(k) \ll \mathrm{Re}(k)$. For a Maxwellian electron distribution function, such root does not exist when $\omega \ll \omega_p$. However, electron acoustic waves can exist if the plasma contains two groups of electrons which have very different temperatures [26]. The wave phase velocity is $\omega/k = \sqrt{n_c/n_h}\sqrt{T_h/m}$, where $n_c$ and $n_h$ are the electron densities of cold and hot electrons, respectively, and $T_h$ is the temperature of the hot electrons. Electron acoustic waves are strongly damped by the hot electrons, unless $n_c \ll n_h$ and $T_c \ll T_h$, where $T_c$ is the electron temperature of the cold electrons [26]. In the opposite limit, $n_c > 4n_h$, electron acoustic waves do not exist [26]. In capacitively coupled discharges, the electron population stratifies into two populations of cold and hot electrons, as has been observed in experiments [27] and simulation studies [28], [29]. Cold electrons trapped by the plasma potential in the discharge center do not interact with the large electric fields in the sheath region and have a low temperature. Moreover, because of the nonlinear evolution of plasma profiles, the cold electron density is much larger than the hot electron density [28]. Therefore, weakly damped electron acoustic waves do not exist in the plasma of capacitively coupled discharges. Reference [13] used the fluid equation and neglected the effect of collisionless dissipation, thus arriving at the incorrect conclusion about the existence of weakly damped electron acoustic waves.

The power deposition is given by the sum of the power transferred to the electrons by the oscillating rigid barrier in the sheath region and by the electric field in the transition region

$$P_{\rm tot} = P_{\rm sh} + P_{\rm tr}. \tag{30}$$

Note that $P_{\rm tr}$ can be negative. Calculations making use of the Vlasov equation yield [14]

$$P_{\rm tot} = -\int_0^\infty muD_u(u)\frac{df_0}{du}\,du \tag{31}$$

where

$$D_u(u) = \frac{u|du|^2}{4} \tag{32}$$

is the diffusion coefficient in velocity space, and $du$ is the change in the electron velocity after passing through the transition and sheath regions

$$du = 2iV_b\left[\frac{u'}{u}\frac{n_b}{n_{\rm sh}}\Theta(|u| - u_{\rm sh}) - 1\right] + \frac{eE_t(k = \omega/u)}{u} \tag{33}$$

where $E_t(k)$ is the Fourier transform of the electric field $E_t(x)$. First term describes the velocity acquired by fast electrons ($|u| > u_{\rm sh}$) in collisions with the sheath; the second is due to the bulk electric field $E_b$ and collisions with either the potential barrier $\Phi_{\rm sh}$ or sheath; and the third is due the electric field in the transitional region $E_t(x)$. A plot of $|du|^2/4$ is shown in Fig. 6. Taking into account the electric field in the plasma (both $E_b$ and $E_t$) reduces $|du|$ for energetic electrons ($u > u_{\rm sh}$) and increases $|du|$ for slow electrons ($u < u_{\rm sh}$). *Therefore, the electric field in the plasma cools the energetic electrons and heats the low-energy electrons, respectively*. Similar observations were made in numerical simulations [13]. Fig. 7 shows the dimensionless power density as a function of $n_b/n_{\rm sh}$. Taking into account the electric field in the plasma (both $E_b$ and $E_1$) reduces the total power deposited in the sheath region. Interestingly, taking into account only the uniform electric field $E_b$ gives a result close to the case when both $E_b$ and $E_1$ are accounted for. The electric field $E_1$ redistributes the power deposition from the energetic electrons to the low energy electrons, but does not change the total power deposition (compare lines (a) and (b) in Figs. 6 and 7). Therefore, the total power deposition due to sheath heating can be calculated approximately from (31), taking into account only the electric field $E_b$. This gives

$$P_{\rm tot} \approx -mV_b^2\int_0^\infty u^2\left[\frac{u'}{u}\frac{n_b}{n_{\rm sh}}\Theta(u - u_{\rm sh}) - 1\right]^2\frac{df_0}{du}\,du. \tag{34}$$

The result of the self-consistent calculation of the power dissipation in (34) differs from the non-self-consistent estimate by the

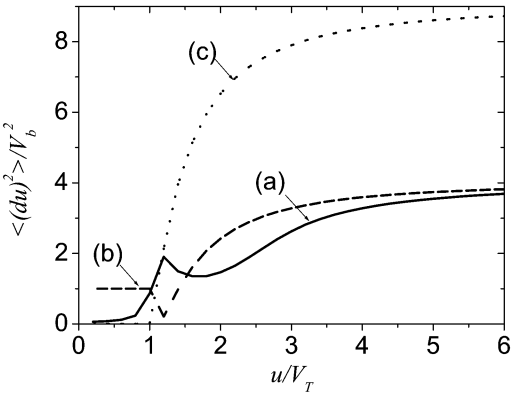


Fig. 6. Plot of the averaged square of the dimensionless velocity kick as a function of the dimensionless velocity for the conditions in Fig. 1, taking into account (a) both $E_1(x)$ and $E_b$—solid line; (b) only $E_b$—dashed line; and (c) no electric field—dotted line.

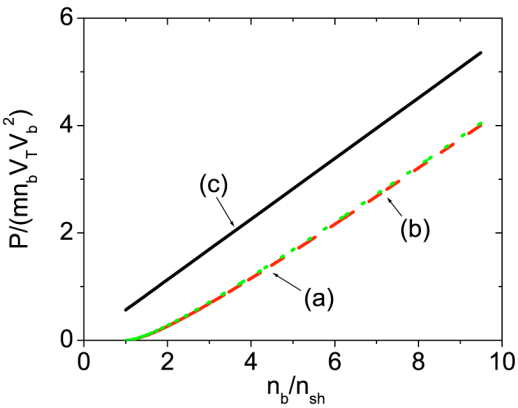


Fig. 7. Plot of the dimensionless power density as a function of the ratio of the bulk plasma density to the sheath density (color online), taking into account (a) both $E_1(x)$ and $E_b$—solid (black) line; (b) only $E_b$—dashed (red) line; and (c) no electric field inside the plasma—dotted (green) line.

last term in (34), which contributes corrections of order $n_{\rm sh}/n_b$ to the main term.

II) Collisionless Heating in Capacitive Sheath Making Use of Nonuniform Ion Density Profile: Based on results of exact linear kinetic theory for the two-step approximation of the ion density profile in sheath, the power dissipation in the sheath can be calculated taking into account more realistic model of ion density profile in the sheath. The ion density profile was calculated analytically in [7], [30], and [31], and is given by a parametric function of the phase of the sheath motion $\phi$

$$n_{\rm sh}(\phi) = \frac{n_b}{H\left(-\frac{3}{8}\sin 2\phi + \frac{1}{2}\phi + \frac{1}{4}\phi\cos 2\phi\right) + 1} \tag{35}$$

where

$$H \equiv \frac{4j^2}{e\omega^2 n_p T}, \tag{36}$$

and $\phi(x)$ profile is

$$x = \frac{V_b}{\omega}\left[1 - \cos\phi + \frac{H}{8}\left(\frac{3}{2}\sin\phi + \frac{11}{18}\sin 3\phi - 3\phi\cos\phi - \frac{1}{3}\phi\cos 3\phi\right)\right]. \tag{37}$$

Note that cgs units are used rather than the MKS units of [7], [30].

The velocity of plasma-sheath boundary is given by current conservation law

$$n_{\rm sh}(\phi)V_{\rm sh}(\phi) = n_b V_{b0}\sin\phi. \tag{38}$$

The outlined above concept of diffusion in energy can be used to calculate the power deposition. However, a more conventional arguments making use of (25) give the same results when necessary modifications stemming from the self-consistency requirements are applied, chiefly by the requirement of conservation of the electron current in plasma phase of the sheath.

As discussed above, if the plasma bulk has a uniform density $n_b$, far a way from the sheath (on distances larger than $V_T/\omega$), the electron flow velocity is $V_b(t)$ given by (27) and the electric field $E_b = m/e\, dV_b(t)/dt$. In the frame of reference moving with the electron mean flow velocity $V_b(t)$, there is no force acting on the electrons and there is no current, as discussed above. This makes it convenient to consider interaction with the sheath in this reference frame. An electron with velocity $u'$ acquires velocity $-u'+2(V_{\rm sh}-V_b)$ after collision with the sheath, in the reference frame moving with $V_b(t)$. If ion density profile is uniform in the sheath, $V_{\rm sh} = V_b$, and there is no change in electron energy if $n_{\rm sh} = n_b$, as discussed above. If $n_{\rm sh} < n_b$, $V_{\rm sh} > V_b$ and the reflection from the moving wall produces an electron current. To conserve the electron current in plasma, an electric field $E_t$ is generated on distances of order $V_T/\omega$ similar to the one calculated above for the two-step profile of ion density. It is difficult to calculate this electric field for the general case of nonuniform ion density profile, as it requires solving an integral equation [32]. Instead of direct calculation, the supposition can be used that this electric field does not change the total power balance. This supposition is supported by the result of two step model, that this field redistributes the power from fast electron to slow electrons without changing the total power balance, see Fig. 7. Calculating the power transfer from the sheath electric field to plasma electron in the reference frame moving with $V_b(t)$ gives

$$P_{\rm sh} = \frac{m}{2}\left\langle \int_{-(V_{\rm sh}-V_b)}^{\infty} du'\,[u' + V_{\rm sh} - V_b] \times \left[(2(V_{\rm sh}-V_b)+u')^2 - u'^2\right] f(-u')\right\rangle. \tag{39}$$

The difference between (25) and (39) is that $V_{\rm sh}$ is substituted by $V_{\rm sh} - V_b$ and $u$ to $u'$ of (29) where slowing of an electron energy by the ambipolar potential is taken into account. Note

that $f(-u')$ is stationary EDF in the reference frame moving with $V_b(t)$. Equation (39) gives

$$P_{\rm sh} = 2m\left\langle \int_0^\infty du'(V_{\rm sh}-V_b)[u'+V_{\rm sh}-V_b]^2 f(-u')\right\rangle \tag{40}$$

and accounting that $\langle (V_{\rm sh}-V_b)^n\rangle = 0$ for $n = 1, 3$, (40) becomes

$$P_{\rm sh} = 4m\left\langle \int_0^\infty du'u'(V_{\rm sh}-V_b)^2 f(-u')\right\rangle. \tag{41}$$

Note that (41) could have been obtained making use of energy diffusion concept given by (31) and (32) with velocity kick

$$du = 2i(V_{\rm sh}-V_b)\frac{u'}{u}. \tag{42}$$

Here, the velocity kick $du$ does not account for the electric field $E_t$ and, in contrast to two-step model, bulk electrons can reach the sheath region—there is no a potential barrier in front of the sheath, rather it spreads out across entire width of the sheath. These two effects account for the difference between (33) and (42). Note that there is an additional heating due to $E_b$ and the electron collision with the ambipolar potential when electrons do not reach the moving plasma-sheath boundary. In case of sharp boundary assumed in two-step model, it yields velocity kick with the amplitude $2V_b$; however, when the ambipolar potential is not steep than the velocity kick is much smaller due to "softness of interaction" [10] $du = 2\int_0^\infty E_b v_x(x)\sin\omega t e^{-\nu t}dt/u < 2V_b$ [11], [52]. Here, $v_x(x) = \sqrt{u^2 - 2e\Phi(x)/m}$ is the electron velocity determined by the ambipolar potential in the plasma phase of the sheath. A further detailed study is needed to quantify this effect, which should involve cumbersome calculations for $E_t(x)$ profile and heating accounting for both $E_t(x)$ and $E_b$, the first attempt has been recently initiated [32].

Assuming a Maxwellian EEDF $f(u) = n_b\exp(-mu^2/2T_e)1/\sqrt{2\pi T/m}$ and substituting $u'$ from (29) gives $f(u') = n_{\rm sh}\exp(-mu'^2/2T_e)1/\sqrt{2\pi T/m}$. Substituting $V_{\rm sh}$ from (38) into (41) gives

$$P_{\rm sh} = m\sqrt{\frac{8T}{\pi m}}n_b V_b^2\left\langle\left(\frac{V_{\rm sh}(\phi)}{V_{b0}}-1\right)^2\sin^2\phi\frac{n_{\rm sh}(\phi)}{n_b}\right\rangle_\phi. \tag{43}$$

The result (43) differs from the result of [7], [30], [31] by substitution of $V_{\rm sh}/V_b$ with $V_{\rm sh}/V_b - 1$. This provides zero heating in case of a uniform ion density profile. Substituting ion density profile [7], [30], and [31]

$$n_{\rm sh}(\phi) = \frac{n_b}{HN(\phi)+1} \tag{44}$$

where

$$N(\phi) = \left(-\frac{3}{8}\sin 2\phi + \frac{1}{2}\phi + \frac{1}{4}\phi\cos 2\phi\right) \tag{45}$$

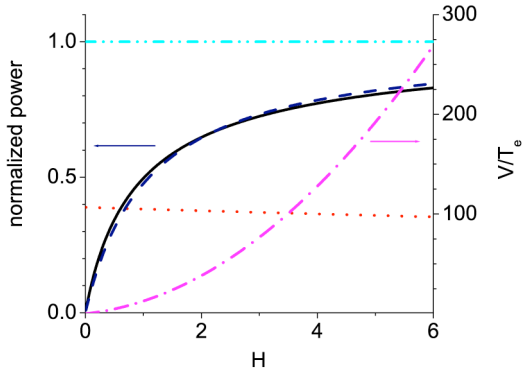


Fig. 8. Plot of the averaged power density in CCP sheath as a function of ratio of the plasma bulk density to the sheath density (color online). Dimensionless power deposited in one sheath $G(H)$ normalized according to (46) as a function of ion density nonuniformity in the sheath $H = 8n_b/5\pi n_{\rm sh0}$. Predictions of (47) are shown in solid (black) line and fit $G(H) = H/(H+1.1)$—dashed (blue) line; results of ([7], [30])—dashed–double-dotted (cyan) line and $G(H) = 70/3(H+60)$ of ([15])—dotted (red) line. Dashed–dotted (magenta) line shows amplitude of the RF voltage on sheath normalized on electron temperature $V/T_e = \pi H[8+125\pi H/48]/4$ [7], [30].

into (43) gives

$$P_{\rm sh} = \frac{3\pi}{32}m\sqrt{\frac{8T}{\pi m}}n_b V_{b0}^2 H G(H) \tag{46}$$

where

$$G(H) = \left\langle\frac{N(\phi)^2\sin^2\phi}{N(\phi)+1/H}\right\rangle \simeq \frac{H}{H+1.1}. \tag{47}$$

In the limit of large $H$, (46) coincides with the result of [7], [30]. Note that power dissipation is determined by the region where ion density is the smallest, i.e., at the electrode $\phi = \pi$, $n_{\rm sh0} \equiv n_{\rm sh}(\pi) = n_b 8/5\pi H$ and

$$P_{\rm sh} = \frac{3}{20}m\sqrt{\frac{8T}{\pi m}}n_{\rm sh0}V_{\rm sh0}^2 G(H). \tag{48}$$

Functions $G(H)$ obtained by different theories are shown in Fig. 8. For usual CCP operation conditions, the capacitive RF bias is of order few hundred volts, $V \sim 200$ V and $V/T_e \sim 50$, which gives $H \sim 2$. The current theory predicts collisionless power deposition by the sheath 70% of the model, which does not account for influence of self-consistent field in the plasma on electron dynamics [5], [7]. The fluid theory of [15] predicts much less about 40% of power deposition compared with Lieberman's model. The fluid theory was verified by the authors' PIC simulations. The suppositions of fluid theory that modification of EDF by the interaction with the sheath can be described by modification of the electron temperature only contradicts the analytical kinetic model in two-step approximation, which predicts EDF is close to Lieberman's model plus perturbation caused by the transitional electric field $E_t$. Such a big difference between various theories and simulation results requires additional verification, as well as, detailed comparison with experimental data. However, the direct comparison with the experimental data is complicated by a non-Maxwellian EEDF in

CCP discharges and requires the self-consistent kinetic modeling similar to one performed in [29], [33].

A future development should provide a self-consistent, kinetic analysis with a nonuniform ion density profile $n_i(x)$ and is being now underway [34]. Such a study has been currently performed only for inductively coupled discharges.

## III. Penetration of the RF Electric Field Into an Inductively Coupled Plasma

Low-pressure inductively coupled RF discharges are often operated in the nonpropagating regime, when the driving RF field penetrates into plasma only within a skin layer of width $\delta$ near the antenna, i.e., exhibits a skin effect. Not only the RF field, but, in this case, also the resulting induced electric current is concentrated near the surface of the plasma. Depending on the local, or nonlocal nature of the relation between the electric current $j$ induced in plasma and the RF electric field $E$, the skin effect is called *normal*, if the dependence of the current on the electric field is local, or *anomalous*, if the dependence of the current on the electric field is nonlocal [35]–[37].

To differentiate between the two regimes of the skin effect, it is convenient to introduce the nonlocality parameter [36] $\Lambda = (\lambda/\delta_0)^2$, where $\lambda \equiv v_T/(\omega^2+\nu^2)^{1/2}$ is the effective electron mean free path and

$$\delta_0 = \frac{c}{\omega_p(1+\nu^2/\omega^2)^{1/4}} \tag{49}$$

is the depth of the normal skin effect. The parameter $\Lambda$

$$\Lambda = \frac{v_T^2\omega_p^2}{\omega^2 c^2(1+\nu^2/\omega^2)^{1/2}} \tag{50}$$

is a fundamental measure of plasma current nonlocality. In the local limit $\Lambda \ll 1$, the effective mean free path is small compared with the skin depth $\lambda \ll \delta$, and the current density at a particular point in space can be considered as a function of the electric field at the same point $\mathbf{j}(\mathbf{x}) = \sigma(\mathbf{x})\mathbf{E}(\mathbf{x})$ (Ohm's law). In the opposite limit $\lambda \gg \delta$, the mean free path exceeds the skin depth $\lambda \gg \delta$, the relation between the current and the field $\mathbf{j}(x) = \int \underline{\sigma}(\mathbf{x},\mathbf{x}')\mathbf{E}(\mathbf{x}')d\mathbf{x}'$ is no longer local, because the conductivity $\sigma(\mathbf{x},\mathbf{x}')$ has a spatial dispersion.

The penetration of the RF electric field into the plasma is described according to Faraday's and Ampere's laws

$$\boldsymbol{\nabla}\times\mathbf{E} = -\frac{1}{c}\frac{\partial\mathbf{B}}{\partial t} \tag{51}$$

$$\boldsymbol{\nabla}\times\mathbf{B} = \frac{1}{c}\frac{\partial\mathbf{D}}{\partial t} + \frac{4\pi}{c}\mathbf{j}. \tag{52}$$

For a transverse harmonic electric field in 1-D geometry $E_y(x)e^{-i\omega t}$, Faraday's and Ampere's laws give

$$\left(\frac{\partial^2}{\partial x^2} + \frac{\omega^2}{c^2}\right)E_y = -\frac{4\pi i\omega}{c^2}j_y \tag{53}$$

where the current $j$ is the plasma electron current $j_y = j_{ey}$ (the ions are considered stationary), which has to be calculated making use of the electron kinetic equation, similar to the case of the penetration of the longitudinal electric field into the plasma described in the previous section.

### A. Normal Skin Effect

In the limit of the normal skin effect ($\Lambda \ll 1$), the electron thermal motion can be neglected. The electron flow velocity $V_{ey}$ may be obtained from Newton's law taking into account the drag force due to electron neutral collisions

$$m\frac{\partial}{\partial t}V_{ey} = -eE_y - \nu V_{ey}. \tag{54}$$

This gives for the electron current ($j_{ey} = -en_eV_{ey}$) the Ohm's law relationship

$$\mathbf{j}_e(x) = \sigma_e\mathbf{E}(x) \tag{55}$$

where

$$\sigma_e = \frac{e^2n_e}{m(\nu - i\omega)}. \tag{56}$$

The plasma current density is proportional to the electric field at the same point of space with a proportionality coefficient that is the complex conductivity of the cold plasma. Substituting Ohm's law (55) with plasma conductivity from (56) into (53) gives the solution of the wave equation

$$E_y = E_{y0}e^{-\alpha x} \tag{57}$$

where $\alpha = \sqrt{-4\pi i\omega\sigma_e/c^2}$. Here, we neglected small terms associated with the displacement current in the limit $\omega \ll \omega_p$, which is valid for the most plasma parameters in ICP discharges. The electric field can be equivalently expressed as

$$E_y(x,t) = E_{y0}e^{-\cos(\epsilon/2)x/\delta_0}\cos[\omega t - \sin(\epsilon/2)x/\delta_0] \tag{58}$$

where $\delta_0$ is the normal skin depth in (49), and $\epsilon = \arctan(\nu/\omega)$.

### B. Anomalous Skin Effect

The case of anomalous skin effect ($\Lambda \geq 1$) for low-pressure inductively coupled plasmas is more complicated compared to the case of normal skin effect, and requires a more elaborate mathematical and numerical treatment to uncover its intrinsic complexity. In the limit $\Lambda \gg 1$, the electron mean free path is large compared with the skin depth, and the electron current is determined not by the local RF electric field (Ohm's law), but rather is a function of the whole profile of the RF electric field over distances of order $\lambda$. Therefore, a rather complicated nonlocal conductivity operator has to be determined for the calculation of the RF electric field penetration into the plasma.

In the case of a uniform plasma, the Vlasov and Maxwell equations can be solved by applying a Fourier transform

[35]. For a transverse harmonic electric field in 1-D geometry $E_y(x)e^{-i\omega t}$, a spatial Fourier harmonic of the current $j_{yk}\exp(-ikx)$ simplifies to become [37], [38]

$$j_{yk} = \frac{e^2 n}{imkV_T} Z\left(\frac{\omega}{kV_T}\right) E_{yk}. \tag{59}$$

Details of the solution are given in Appendix C. The electric field profile is given by the inverse Fourier transform of (53)

$$E_y(x) = \frac{2i\omega}{c^2} I \int_{-\infty}^{\infty} \frac{e^{ikx}}{k^2 - \omega^2 \varepsilon_t(\omega,k)/c^2}\, dk. \tag{60}$$

Here, $I$ is the surface current in the antenna and $\varepsilon_t(\omega,k)$ is transverse plasma permittivity, which for a Maxwellian EEDF is given by [3]

$$\varepsilon_t(\omega,k) \simeq 1 + \frac{\omega_p^2}{\omega^2}\frac{\omega}{v_T|k|} Z\left(\frac{\omega}{v_T|k|}\right). \tag{61}$$

Note the module sign as an argument of the plasma dispersion function. It reflects the proper symmetry of the continued electric field profile into semi-plane $x<0$ and also the proper pole position of the plasma dispersion function [2], [11], [52]. Neglecting the module sign results in erroneous results.

The solution for the electric field (60) has been described in many reviews and textbooks [3], [8], [11], [52], [37]. Here, we only focus on a property of the solution (60) not commonly acknowledged in the literature.

In the limit $\Lambda \gg 1$ or $\delta \ll v_T/\omega$, the plasma dielectric function can be substituted by its limiting value at small arguments $Z \simeq i\sqrt{\pi}$. Introducing the anomalous skin depth

$$\delta_a \equiv \frac{c}{\omega_p}\left(\frac{\omega_p v_T}{\omega c\sqrt{\pi}}\right)^{1/3} \tag{62}$$

and substituting $Z \simeq i\sqrt{\pi}$ into (61) and into (60) gives

$$E_y(x) = \frac{2i\omega}{c^2} I \int_{-\infty}^{\infty} \frac{e^{ikx}}{k^2 - i/|k|\delta_a^3}\, dk. \tag{63}$$

The integral in (63) cannot be calculated analytically, but it can be transformed into an integral in the complex $k$ plane by substituting $|k| = \sqrt{k^2}$. The contour of the integration should encompass branch point of the function $\sqrt{k^2}$ and has to come around the imaginary $k$ axis. This gives [11], [52]

$$E_y(x) = E_0 \frac{(i\sqrt{3}+1)}{3\gamma_1}\exp\left(-\frac{x\gamma_2}{\delta_a}\right) + \frac{E_0}{3\gamma_1}\exp\left(-\frac{x}{\delta_a}\right) \tag{64}$$

$$-\frac{2iE_0}{\pi\gamma_1} P\int_0^{\infty} \frac{\xi\exp(-x\xi/\delta_a)}{1-\xi^6}\, d\xi. \tag{65}$$

where $\gamma_1 = 2(\sqrt{3}+i)/3\sqrt{3}$, $\gamma_2 = (1-i\sqrt{3})/2$ and $E_0$ is the electric field at the plasma boundary at $x=0$, $P$ stands for principal value of the integral. The last term represents the contribution of the integral around the imaginary $k$-axis and the exponential terms originate from the poles. The electric field at $x=0$ can be calculated analytically

$$E_0 = \frac{4i\omega I}{c^2}\frac{\pi(\sqrt{3}+i)\delta_a}{3^{3/2}}. \tag{66}$$

From Maxwell's equations it follows that the magnetic field near the coil is $B|_{0+} = 2\pi I/c$. Correspondingly, the derivative of the electric field at the plasma boundary is

$$\left.\frac{dE_y}{dx}\right|_{x=0} = -\frac{2\pi i\omega}{c^2} I. \tag{67}$$

The characteristic decay length of the electric field can be introduced as [40], [41]

$$\delta_s = \frac{E_0}{-dE_y/dx} = \frac{2}{3}(1+i/\sqrt{3})\delta_a. \tag{68}$$

The electric field profile from (69) is compared in Fig. 9 with the exponential profile

$$E_y(x) = E_0\exp[-x\mathrm{Re}(1/\delta_s)]. \tag{69}$$

A more conventional plot of the amplitude and phase of the electric fields is shown in Fig. 10.

### *C. Spatially Averaged Electric Field, $\int_0^{\infty} E_y dx \to 0$ in the Limit of a Strong Anomalous Skin Effect $\Lambda \to \infty$*

The most apparent difference between the anomalous skin effect and the normal skin effect is that the amplitude of the RF field is nonmonotonic in the limit of anomalous skin effect and monotonic (exponential) for the normal skin effect. Moreover, in the case of the extremely anomalous skin effect, in the limit $\Lambda \gg 1$, the spatially averaged RF electric field tends to zero [11], [52]

$$\int_0^{\infty} E_y\, dx \to 0, \quad \Lambda \to \infty. \tag{70}$$

In other words, the phase of the electric field changes by $\pi$ inside the skin layer, see Fig. 10(b). The spatially averaged electric field is given by the Fourier component at $k=0$, i.e.,

$$\int_0^{\infty} E_y dx = \pi E(k=0). \tag{71}$$

Substituting the Fourier component of the electric field from (60) into (71) gives

$$\int_0^{\infty} E_y(x)\, dx = \frac{2\pi i\omega I}{c^2}\frac{1}{\omega^2\varepsilon(\omega)/c^2} \tag{72}$$

and

$$\frac{\int_0^{\infty} E_y(x)\, dx}{|E_0|\delta_a} = \frac{3^{3/2}\pi^{1/3}}{\Lambda^{1/3}}. \tag{73}$$

From (73), it is evident that as the nonlocality parameter tends to infinity, the averaged electric field tends to zero. This property of the electric field profile is consistent with nonlocality of the

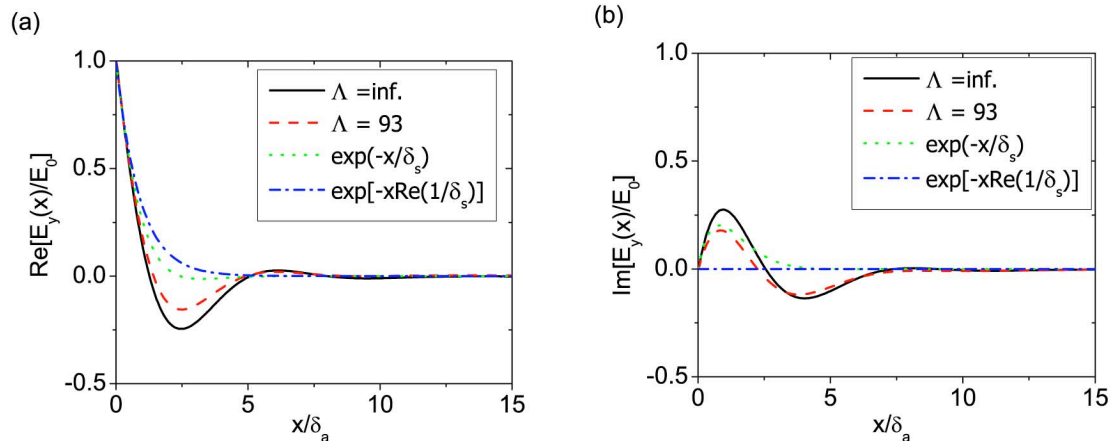


Fig. 9. Plot of the RF electric field as a function of the normalized coordinate $x/\delta_a$ (color online). Solid (black) curve corresponds to the solution in the limit $\Lambda = v_T\omega_p/c\omega = \infty$; dashed (red) line—$\Lambda = 93$ (plasma parameters $\mathrm{n} = 10^{11}$ cm$^{-3}$, $\mathrm{T}_e = 3$ eV, $\mathrm{f} = 1$ MHz). Dotted (green) and dash–dotted (blue) lines shows the skin approximation in (68) and (69): (a) real and (b) imaginary part of the electric field.

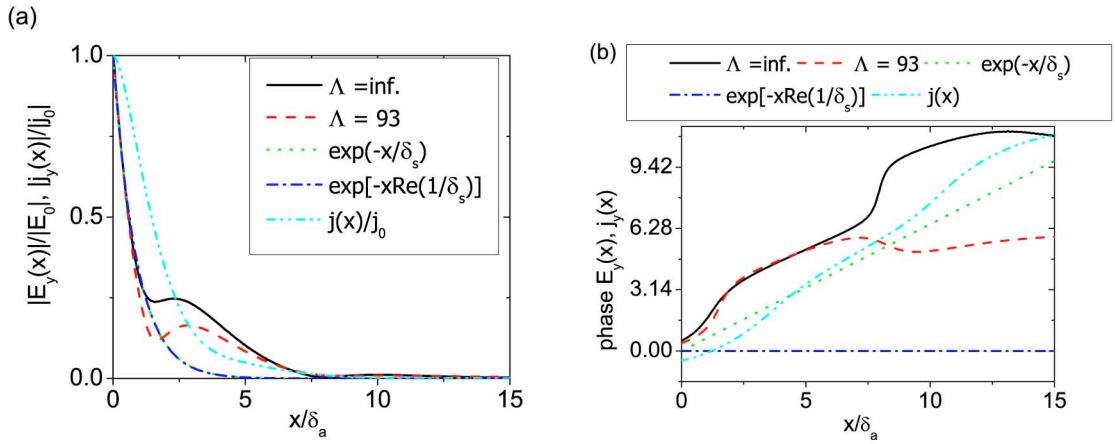


Fig. 10. Plot of the RF electric field and electron current as a function of the normalized coordinate $x/\delta_a$ (color online). Same profiles as in Fig. 9, shown are (a) amplitude, and (b) phase with respect to the phase of the electric field generated by the field in vacuum.

electron current. The electric field profile and the current profile are coupled to each other by (53). Therefore, the main part of the current and the electric field should decay on distances of order $\delta_a$, see Fig. 10. However, if the electric field profile has a nonzero average, the fast electrons will pick up a velocity kick from the skin layer and will transport the current over distances of order $v_T/\omega \gg \delta_a$, where the electric field vanishes. This would contradict Maxwell's equations. *Therefore, zero average of the electric field is necessary and an important property of the electric field profile in the limit of the extreme anomalous skin effect* $\Lambda \to \infty$.

The penetration length is defined in textbooks [40], [41] as

$$\lambda_E = \frac{\int_0^\infty E_y(x)dx}{E_0}. \tag{74}$$

From the above discussion, it follows that this definition is confusing, because in the limit of the anomalous skin effect the above defined penetration length is $\lambda_E \ll \delta_a$ and is not a good measure of penetration length of the electric field. A better definition would be

$$\lambda_{|E|} = \frac{\int_0^\infty |E_y(x)|dx}{|E_0|}. \tag{75}$$

In the limit of the strong anomalous skin effect, i.e., $\Lambda \gg 1$, numerical calculation gives

$$\lambda_{|E|} = 1.64\delta_a. \tag{76}$$

From Fig. 10, it is evident that in the region $x \lesssim 2\delta_a$ the amplitude of the electric field can be approximated by the exponential profile in (69) with the decay length

$$\delta_e = \frac{1}{\mathrm{Re}(1/\delta_s)} = \frac{8}{9}\delta_a. \tag{77}$$

Note that the penetration length defined by (75), $\lambda_{|E|}$ is nearly twice as large as the initial decay length of the electric field

amplitude near the plasma-wall boundary $\delta_e$. This is due to the pronounced long tail in the profile of the electric field.

Similarly, if we introduce the penetration length of the current

$$\lambda_{|j|} = \frac{\int_0^\infty |j_y(x)|dx}{|j_0|} \tag{78}$$

numerical simulation gives

$$\lambda_{|j|} = 1.87\delta_a \approx \lambda_{|E|}. \tag{79}$$

This result contradicts to claim of [40] and [42], that the magnetic field and current penetration lengths are much longer than the electric field penetration length. This claim is the result of an inaccurate definition of the penetration length.

In an attempt to reduce the phenomenon of the anomalous skin effect to the normal skin effect, many authors have substituted the correct profile of the electric field in (64) by an exponential profile $E_0 \exp(-x/\delta_e)$ with some fitting procedure for $\delta_e$ [43]–[45], [53]. By doing so, the property of the electric field in the limit of anomalous skin effect in (70) is violated. This leads to overestimation of the electron heating [11], [52]. Under the conditions of the anomalous skin effect $v_T \gg \delta_a\omega$, electrons acquire a velocity kick

$$\Delta v_y = -\frac{2e}{mv_x}\int_0^\infty E_y(x)\,dx. \tag{80}$$

If $E_y(x)$ satisfies the condition in (70), the electron velocity kick after passing through the skin layer is much smaller than in the case of an exponential electric field profile, which does not satisfy the property $\int_0^\infty E_y dx \to 0$, as $\Lambda \to \infty$.

### *D. Analytical Separation of the Electric Field Profile Into an Exponential Part and a Far Tail*

Consider an exponential profile of the electric field in a plasma

$$E_y(x,t) = E_{y0}\exp(-k_p x - i\omega t) \tag{81}$$

where $k_p$ is a real positive number. The velocity perturbation in this electric field becomes

$$\Delta v_y(x,t) = -\frac{e}{m}\int_{-\infty}^{t} d\tau E_y[x(\tau),\tau]. \tag{82}$$

The velocity kick $\Delta v_y$ can be separated into a purely exponential part and a nonexponential part. Substituting the electron trajectory $x(\tau) = x - v_x(t-\tau)$ for $v_x < 0$ gives

$$\Delta v_y(x,t) = -\frac{e}{m}\frac{Ey_0}{-k_p v_x - i\omega}\exp(-k_p x - i\omega t). \tag{83}$$

For $v_x > 0$, the velocity acquired by an electron can be represented as the difference between the velocity kick acquired after a full pass through the skin layer and the contribution from the part of the skin layer $[x;\infty]$, i.e.,

$$\Delta v_y(x,t) = -\frac{e}{m}\left[\int_{-\infty}^{\infty} - \int_t^\infty\right] d\tau E_y[x(\tau),\tau]. \tag{84}$$

The second part of the integral $(\Delta v_y^e)$ in (84) gives an exponential profile for the velocity kick, similar to (83)

$$\Delta v_y^e(x,t) = -\frac{e}{m}\frac{E_{y0}}{-k_p v_x - i\omega}\exp(-k_p x - i\omega t), \quad v_x > 0. \tag{85}$$

The first part of the integral $(\Delta v_y^{\text{in}})$ in (84) gives

$$\Delta v_y^{\text{in}} = \Delta v_y^\infty e^{-i\omega(t - x/v_x)} \tag{86}$$

$$\Delta v_y^\infty = -\frac{e}{m}E_{y0}\left(\frac{1}{-i\omega + k_p v_x} - \frac{1}{-i\omega - k_p v_x}\right). \tag{87}$$

Here, $\Delta v_y^\infty$ is the velocity kick acquired during the pass through the entire skin layer. The time $t - x/v_x$ corresponds to the moment the electron collides with the wall.

Substituting $\Delta v_y^e(x,t)$ from (83) and (85) gives for the exponential part of the current

$$j_y^e = [-e\int \Delta v_y \frac{\partial f}{\partial v_y} v_y\,d\mathbf{v} \tag{88}$$

$$j_y^e = \frac{e^2}{m}E_{y0}e^{-i\omega t - k_p x}\int \frac{1}{-k_p v_x - i\omega}\frac{\partial f}{\partial v_y}v_y\,d\mathbf{v} \tag{89}$$

or, after integration, the exponential profile of the current becomes

$$j_y^e = \frac{e^2}{m}E_{y0}e^{-i\omega t - k_p x}\frac{n}{k_p V_T}Z\left(\frac{i\omega}{k_p V_T}\right)^*. \tag{90}$$

The asterisk denotes the complex conjugate. Note that (90) can be derived from (59) with the substitution $k = ik_p$ and by accounting for the following property of the dispersion function [4]

$$Z(\xi^*) = -Z(-\xi)^*. \tag{91}$$

The exponential part of the profile should satisfy Maxwell's equation (53). This gives an expression for $k_p$

$$k_p^2 = \frac{\omega^2}{c^2} + \frac{\omega_p^2}{c^2}\frac{i\omega}{k_p V_T}Z\left(\frac{i\omega}{k_p V_T}\right)^*. \tag{92}$$

Note that because $Z$ in (92) has only purely imaginary and positive parts, $k_p$ is a real positive number, as it was assumed to be.

The nonexponential part of the electron velocity kick in (86) generates a nonexponential part of the current profile, which decays over a spatial scale of order $V_T/\omega$ due to the phase mixing, as the phase of the velocity kick $\omega(t - x/v_x)$ in (86) is different for electrons with different $v_x$. The current and electric field profiles are essentially nonexponential, similar to (4) for longitudinal velocity kicks, as discussed above. In contrast to

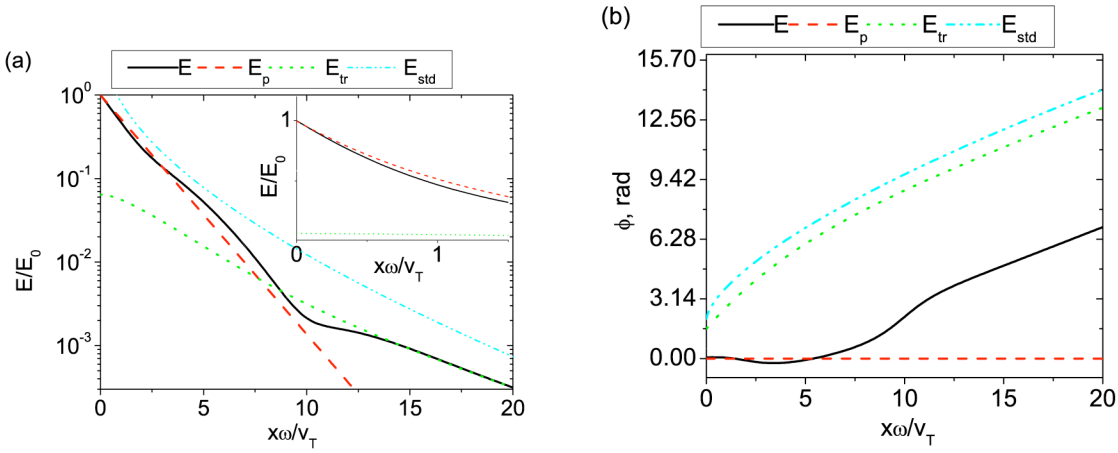


Fig. 11. Plot of the RF electric field as a function of the normalized coordinate $x\omega/V_T$ for plasma parameters $n = 10^{11}$ cm$^{-3}$, $T_e = 3$ eV, $f = 13.56$ MHz (color online). Shown are (a) the amplitude and (b) the phase. Solid lines show the exact electric field profile $E(x)$ calculated according to (60); dashed (red) line, the exponential part of the electric field $E_p(x) = E_0 \exp(-k_p x)$ with $k_p$ from (92); dotted line (green), the difference of the two $E_t(x)$; and, chain (cyan) line, $E_{std}(x)$ shows the asymptotic calculation for $E_t$ in (C22). Subscript $y$ is omitted in the electric field.

the test particle case, the electric field is determined by combination of two effects: phase mixing of the current generated by the velocity kicks of exponential part of the electric field and the plasma screening of this currents as $V_T/\omega > c/\omega_p$. As a result, the analytical expression for nonexponential part is rather complicated.

Details of the exact analytical calculation of the electric field profile separation is given in Appendix C. Applying a procedure similar to that of Landau's treatment [2] for the longitudinal electric field, the integral in $k$ space in (60) can be separated into an integral over an analytic function in the region $k \in [-\infty, \infty]$ and an integral over some nonanalytic function in the region $k \in [0, \infty]$. To do so, the plasma permittivity has to be analytically continued from the real axis $k < 0$, $\mathrm{Im}k = 0$, into the complex $k$ plane, see Appendix C for details. The first integral can be readily calculated using the theory of residues. In the upper half-plane of the complex $k$, there exists only one pole of the analytically continued function of the plasma permittivity continued from $k < 0$. The value of the pole is equal to $ik_p$, given by (92).

In the limit $\omega \gg k_p V_T$, $Z(\zeta) = -1/\zeta$, where $\zeta = i\omega/k_p V_T$. Substituting this value for the plasma dielectric function into (92) yields $k_p = \omega_p/c$, i.e., the normal skin layer length $1/k_p = \delta_0$ in (49) for $\nu \ll \omega$ and $\omega \ll \omega_p$. Fig. 11 shows the profile of the electric field for the same typical ICP parameters: plasma density $n = 10^{11}$ cm$^{-3}$, electron temperature $T_e = 3$ eV, and discharge frequency $f = 13.56$ MHz (color online). Shown are the exact electric field profile $E_y(x)$ calculated according to (60), the exponential part of the electric field

$$E_{yp}(x) = E_0 \exp(-k_p x) \tag{93}$$

with $k_p$ from (92), and the difference of the two

$$E_{yt}(x) = E_y(x) - E_{yp}(x) \tag{94}$$

and the asymptotic calculation for $E_{yt}(x)$ in (C22) $E_{\mathrm{ystd}}(x)$. For these plasma parameters, the skin effect is neither normal nor anomalous: $\omega/k_p V_T = 1.52$. Notwithstanding the fact that the parameter $\omega/k_p V_T$ is of order unity, the main part of the electric field is close to the exponential profile in (93) with $k_p$ from (92), $E_y(x) \approx E_{yp}(x)$. As evident from Fig. 11, the nonexponential part is small, $E_{yt}(x) \ll E_{yp}(x)$, everywhere where the electric field is substantial, or up to distances five times of skin depth, for $x < 5/k_p = 7.5 V_T/\omega$ . The tail of the electric field profile for $x > 7V_T/\omega$ is nonexponential and dominated by $E_{yt}(x)$.

In the limit of the anomalous skin effect $\omega/k_p V_T \ll 1$, $Z(\zeta) = i\sqrt{\pi}$, where $\zeta = i\omega/k_p V_T$. Substituting this value for the plasma dielectric function into (92) yields $k_p = 1/\delta_a$, which is very close to the skin impedance approximation in (69) which corresponds to $k_p = 9/8\delta_a$—a 12% difference. As a result, the exponential profile in (93) approximates well the exact profile of the electric field over distances within a few skin depths even in the limit of the strong anomalous skin effect, as is evident in Fig. 12. However, the nonexponential part $E_{yt}(x)$ dominates $E_{yp}(x)$ at $x > V_T/\omega$ in accord with the requirement in (70).

### E. Surface Impedance

An important plasma characteristic is the surface impedance, which is given by the ratio of the electric field to the RF magnetic field or the coil current at the plasma boundary [3]

$$\mathbb{Z} = \left.\frac{E}{B}\right|_{x=0} \tag{95}$$

where

$$B|_{x=0} = \frac{2\pi}{c} I \tag{96}$$

is the magnetic field near the antenna. The total power $P$ deposited per unit area into the plasma is determined by the energy

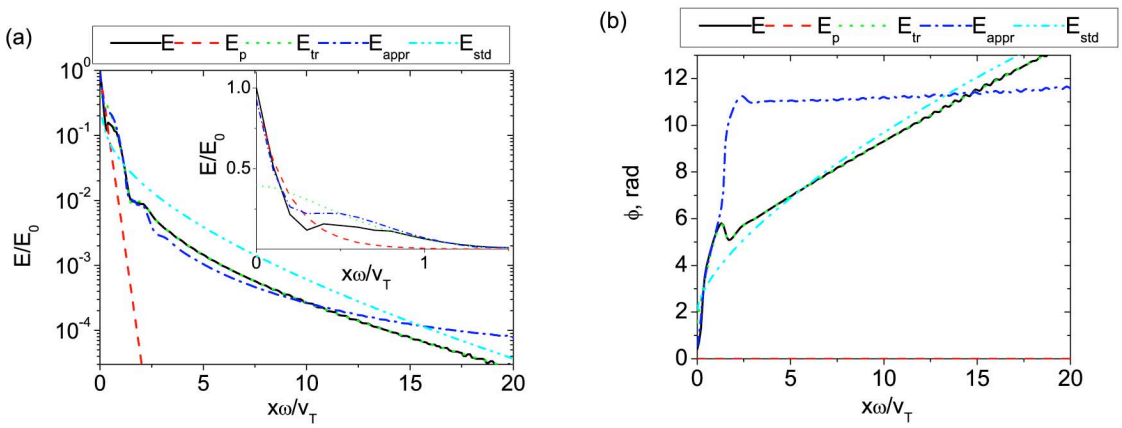


Fig. 12. Plot of the RF electric field as a function of the normalized coordinate $x\omega/V_T$ for plasma parameters $n = 10^{11}$ cm$^{-3}$, $T_e = 3$ eV, $f = 1$ MHz, similar to Figs. 9 and 10. Shown are (a) amplitude and (b) phase. Solid lines show the exact electric field profile $E(x)$ calculated according to (60); dashed (red) line, the exponential part of the electric field $E_p(x) = E_0 \exp(-k_p x)$ with $k_p$ from (92); dotted line (green) the difference of the two $E_t(x)$; chain (blue) line represents the limiting case of strong anomalous skin effect $\Lambda \to \infty$ $E_{\rm appr}(x)$, and dashed and double dotted (cyan) line shows $E_{std}(x)$, the asymptotic calculation for $E_t$ in (C22). Subscript $y$ for the electric fields is omitted.

flux dissipated into the plasma or the time-averaged Poynting vector

$$P = \langle S_x \rangle = \frac{1}{2}\frac{c}{4\pi}\mathrm{Re}(EB^*). \tag{97}$$

Substituting the electric field from (95) and the magnetic field (96) into (97) relates the power to the real part of the surface impedance

$$P = \frac{\pi}{2c} I^2 ReZ. \tag{98}$$

The imaginary part of the surface impedance describes the plasma inductance.

The surface impedance can also be used to estimate the penetration length in the surface impedance approximation given by (68). Substituting the electric field from (95) and the magnetic field (96) into (68) relates the penetration depth and the surface impedance

$$\delta_s = \frac{c\mathbb{Z}}{i\omega}. \tag{99}$$

The surface impedance can be calculated making use of (60), [3], i.e.,

$$\mathbb{Z} = \frac{i\omega}{\pi c}\int_{-\infty}^{\infty} \frac{1}{k^2 - \omega^2\varepsilon_t(\omega,k)/c^2} dk, \tag{100}$$

which requires numerical integration. On the other hand, we can use the results of the previous subsection that the main part of the electric field is an exponential function in (93) with $k_p$ given by (92). From (99), the imaginary part of the surface impedance can be obtained substituting $\delta_s = 1/k_p$

$$\mathbb{Z}_p = \frac{i\omega}{ck_p}. \tag{101}$$

A pure exponential profile yields only the imaginary part of the surface impedance. The real part of the impedance can be calculated by computing the power dissipated by electrons from the skin layer [43]

$$P = \frac{m}{4}\int v_x f |\Delta v_y^\infty|^2 \mathbf{dv} \tag{102}$$

where $\Delta v_y^\infty$ is the velocity kick acquired by an electron after passing through the skin layer, which is given by (87). Here, $m(\Delta v_y^\infty)^2/4$ is the temporal average of the electron energy change in the skin layer and $v_x f$ is the electron flux on the wall. Equation (98) becomes

$$\mathrm{Re}Z_p = \frac{2}{c}\omega_p^2 |Z|^2 \int f v_x \left(\frac{k_p v_x}{\omega^2 + (k_p v_x)^2}\right)^2 dv_x. \tag{103}$$

Because the imaginary part of impedance is large compared with its real part, only the imaginary part can be included on the right hand side in (103). Fig. 13 shows the real and imaginary parts of the surface impedance versus the discharge frequency calculated exactly, i.e., making use of (100), and approximately from (101) and (103). Also shown at the top of this figure, is the ratio of the actual skin depth $\delta = 1/k_p$ from (92) to the normal skin depth calculated in the cold plasma approximation $\delta_0$ given by (49). From Fig. 13, it is evident that within 50% accuracy, the impedance calculation can be based on the exponential profile in (93) for discharge frequencies higher than 1 MHz [44]. However, for lower frequencies, the assumption of purely exponential profile leads to overestimation of the electron heating and plasma resistivity up to a factor of 3 for $f \ll 1$ MHz, see Fig. 13. This is because the important property of the electric field profile under the conditions of strong anomalous skin effect in (70) is being violated. Note that at these low frequencies, taking into account a small but finite collision frequency or nonlinear effects may be important.

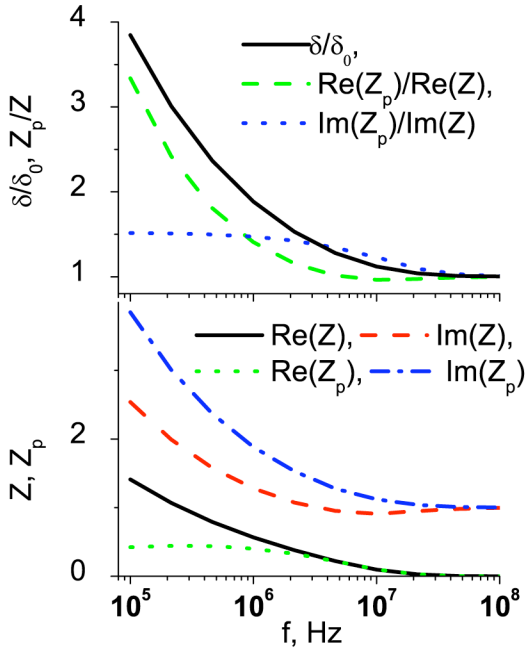


Fig. 13. Plot of the real and imaginary parts of the surface impedance versus discharge frequency calculated exactly making use of (100) and approximately using (101) and (103) in the limit of collisionless plasma $\nu \ll \omega$ (color online). Also shown is the ratio of the actual skin depth $\delta = 1/k_p$ given by (92) to the skin depth calculated in the cold plasma approximation $\delta_0$ (49), (top).

### *F. Anomalous Skin Effect for an Anisotropic Electron Velocity Distribution*

The anomalous skin effect in a plasma with a highly anisotropic electron velocity distribution function (EVDF) is very different from the skin effect in a plasma with the isotropic EVDF. In [47], an analytical solution was obtained for the electric field penetrating into plasma with the EVDF described by a Maxwellian with two temperatures $T_y \gg T_x$, where $y$ is the direction along the plasma boundary and $x$ is the direction perpendicular to the plasma boundary. Under the conditions

$$\frac{v_{Ty}}{\omega} \gg \frac{c}{\omega_p}; \quad \omega_p \gg \omega, \tag{104}$$

the skin layer was found to consist of two distinct regions of width of order $v_{Tx}/\omega$ and $v_{Ty}/\omega$, where $v_{Tx,y} = \sqrt{T_{x,y}/m}$ are the thermal electron velocities in $x$ and $y$ directions, and $\omega$ is the incident electric field frequency. The calculation is based on (60), where the dielectric permittivity has to be modified for an anisotropic EEDF to become

$$\varepsilon_t(\omega,k) = 1 - \frac{\omega_p^2}{\omega^2}\left\{1 - \frac{T_y}{T_x}\left[1 + \frac{\omega}{\sqrt{2}v_{Tx}k} Z\left(\frac{\omega}{\sqrt{2}v_{Tx}k}\right)\right]\right\}. \tag{105}$$

In the case of anisotropic EEDF under conditions in (104), the integral in (60) has two poles and the integration over the branch

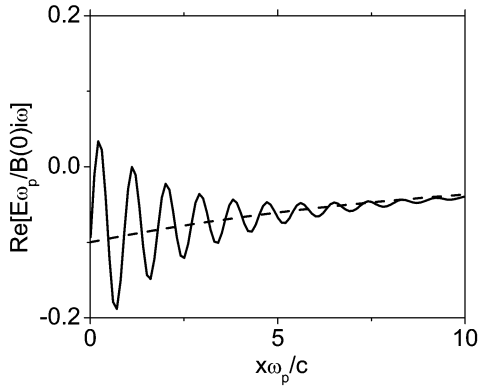


Fig. 14. Electric field in the plasma with $v_{Ty} = 0.1c, \omega = 0.01\omega_p, T_y/T_x = 50$. Solid line shows the real part of the electric field profile obtained from the full solution. Dashed line corresponds to the smooth part of the solution $\sim \exp(-\omega x/v_{Ty})$.

point $k = 0$ does not contribute. As a result, the profile of the electric field is a sum of the two complex exponents

$$E(x) \simeq \frac{\omega}{\omega_p} B(0)\left[-\frac{i\omega c}{\omega_p v_{Ty}} \exp(ik_{p1}x) + \sqrt{T_x/T_y}\exp(ik_{p_2}x)\right] \tag{106}$$

where $k_{p1}$ is given by

$$k_{p1} = i\frac{\omega}{v_{Ty}} \tag{107}$$

and $k_{p2}$ is given by

$$k_{p2} = \frac{\omega_p}{c}\sqrt{T_y/T_x} + i\frac{\sqrt{\pi}\omega}{2\sqrt{2}v_{Tx}}. \tag{108}$$

The profile of the electric field is shown in Fig. 14. The skin layer contains multiple oscillations of the electric field, in striking contrast to the case of an isotropic EEDF.

## IV. Conclusion

We have shown that electrons can transport the plasma current away from the skin layer due to their thermal motion over distances of order $v_T/\omega$. As a result, the width of the skin layer increases when electron temperature effects are taken into account. Anomalous penetration of the RF electric field occurs not only for waves propagating transversely to the plasma boundary (inductively coupled plasmas), but also for waves propagating along the plasma boundary (capacitively coupled plasmas). It was shown that separating the electric field profile into exponential and nonexponential parts yields an efficient qualitative and quantitative description of the anomalous skin effect. Accounting for the nonexponential part of the profile is important for the calculation of the electron heating and the plasma resistivity. For example, the assumption of purely exponential profile leads to overestimation of up to a factor of 3 in the electron heating for $f \ll 1$ MHz, see Fig. 13.

Here, we considered only plasmas with a Maxwellian electron energy distribution function. However, in low-pressure RF

discharges, the EEDF is non-Maxwellian for plasma densities typically lower than $10^{10}$ cm$^{-3}$ [39]. The nonlocal conductivity, and plasma density profiles and EEDF are all nonlinear and nonlocally coupled [46]. Hence, for accurate calculation of the discharge characteristics at low pressures, the EEDF needs to be computed self-consistently [38], [48]–[50]. The effects of a non-Maxwellian EEDF, nonlinear phenomena, the effects of plasma nonuniformity and finite size, as well as influence of the external magnetic field on the anomalous skin effect will be reported in the second part of the review [51].

## Appendix A
## Analytical Derivation of the Current Profile Driven by Velocity Kicks Near the Plasma Boundary

Consider that electrons acquire a velocity kick near the boundary, in the direction perpendicular to the boundary

$$dv_x = \Delta V \cos(\omega t). \tag{A1}$$

The electron velocity at a distance $x$ from the boundary will be determined by the exact moment of the collision with the boundary at a time $t - x/v_x$. The electron current in the plasma is given by integration over all electrons with a distribution function $f(v_x)$

$$j(x,t) = e\Delta V \int_0^\infty f(v_x)\cos(\omega t - \omega x/v_x)\, dv_x. \tag{A2}$$

For a Maxwellian distribution function $f(v_x) = n_0 e^{-v_x^2/v_T}/v_T\sqrt{\pi}$, the current in (A2) takes the form $j(\xi,t) = j_0 A(\xi)\cos[\omega t - \phi(\xi)]$, where $j_0 = en_0\Delta V$ and $A$ and $\phi$ are the amplitude and phase of the current, respectively, and $\xi = \omega x/v_T$. The functions $A$ and $\phi$ are shown in Fig. 1. In the limit $\xi \gg 1$, the integration in (A2) can be performed analytically making use of the method of steepest descent [1]

$$j(\xi,t) = \frac{j_0}{\sqrt{\pi}}\mathrm{Re}\left(e^{-i\omega t}\int_0^\infty e^{-s^2+i\xi/s}ds\right) \tag{A3}$$

where and $s = v_x/v_T$. The integral in (A3) can be calculated in the complex $s$ plane. The stationary phase point is given by $d(-s^2+i\xi/s)/ds = 0$ or $s^3 = -i\xi/2$. This gives the stationary point $s_0 = (-i\xi/2)^{1/3}$. In the neighborhood of this point, the function in the exponent can be expanded as a Taylor series, $-s^2+i\xi/s = -s_0^2+i\xi/s_0-6(s-s_0)^2/2 = -3s_0^2-3(s-s_0)^2$. Integration of the Gaussian gives $\int_0^\infty e^{-3(s-s_0)^2}ds = \sqrt{\pi/3}$. Substituting this into the integration in (A3) yields

$$j(\xi,t) = \frac{j_0}{\sqrt{3}}\mathrm{Re}(\exp[-i\omega t - 3(-i\xi/2)^{2/3}]). \tag{A4}$$

Substituting $(-i)^{2/3} = (e^{-i\pi/2})^{2/3} = e^{-i\pi/3} = \cos(\pi/3) - i\sin(\pi/3) = 1/2 - \sqrt{3}i/2$ into (A4) gives

$$j(\xi,t) = \frac{j_0}{\sqrt{3}}\exp(-3\xi^{2/3}/2^{5/3})\cos(\omega t - 3\sqrt{3}\xi^{2/3}/2^{5/3}). \tag{A5}$$

## Appendix B
## Analytical Derivation of the Longitudinal RF Electric Field Profile Near the Plasma Boundary ($\mathbf{E} \,||\, \mathbf{k}$)

The analytical solution for a longitudinal RF electric field involves solving the Vlasov equation for the electron velocity distribution function (EVDF) $F$

$$\frac{\partial F}{\partial t} + v_x\frac{\partial F}{\partial x} - \frac{e}{m}E_x\frac{\partial F}{\partial v_x} = 0 \tag{B1}$$

together with the Poisson equation

$$\frac{dE}{dx} = 4\pi e\left(n_i - \int_{-\infty}^{\infty} F\, dv_x\right). \tag{B2}$$

In the linear approximation, the EVDF can be split into two parts

$$F(t,x,v_x) = f_0(v_x) + f(t,x,v_x) \tag{B3}$$

where $f_0(v_x)$ describes EVDF of a uniform plasma with uniform ion density $n_e = n_i = n_0$ and $f(t,x,v_x)$ is perturbation of EVDF due a RF electric field. Substituting (B3) into (B1) and (B2) yields the linearized Vlasov–Poisson system of equations

$$\frac{\partial f}{\partial t} + v_x\frac{\partial f}{\partial x} - \frac{e}{m}E_x\frac{df_0}{dv_x} = -\nu f \tag{B4}$$

$$\frac{dE_x}{dx} = -4\pi e\int_{-\infty}^{\infty} f(v_x)dv_x. \tag{B5}$$

In the first (B4), the small collisional term with the collision frequency $\nu \ll \omega$ is taken into account. In [2], Landau solved the linearized Vlasov–Poisson system making use of the Laplace transform for a semi-infinite plasma $x > 0$. However, it is more convenient to apply a Fourier transform to an infinite plasma by artificially continuing the EVDF and the electric field in the semi-plane $x < 0$ [11], [52]. Electrons moving with $v_x < 0$ reflect from the boundary $x = 0$ and change their velocity to $-v_x$. This gives the boundary condition for the Vlasov equation in the semi-plane $x > 0$

$$f(t,0,v_x) = f(t,0,-v_x). \tag{B6}$$

Instead of considering problem in the semi-plane $x > 0$ with the boundary condition in (B6), we can consider the entire plane $x \in [-\infty,\infty]$ by artificially continuing the electric field into the semi-plane $x < 0$. The Vlasov equation is symmetric with respect to a change in variables according to the substitution

$$v_x \to -v_x, \quad x \to -x, \quad E \to -E. \tag{B7}$$

Therefore, electrons at $x = 0$ with $v_x > 0$, which are reflected from the wall can be represented as electrons which came from the semi-plane $x < 0$ and interacted with the electric field

$$E_x(x<0) = -E_x(x>0). \tag{B8}$$

As a result, the electric field has to be continued anti-symmetrically into the semi-plane $x < 0$.

Now we can apply the Fourier transform for the Vlasov-Poisson system of (B4) and (B5). This gives for the components of the EVDF $f_k e^{-i\omega t+kx}$ and the electric field $E_k e^{-i\omega t+kx}$

$$-i(\omega + i\nu - v_x k) f_k - \frac{e}{m} E_k \frac{df_0}{dv_x} = 0 \tag{B9}$$

$$ikE_k + 2E_0 = 4\pi e \int_{-\infty}^{\infty} f_k \, dv_x. \tag{B10}$$

Note that due the fact that the electric field is a discontinuous function, the Fourier transform of the derivative of the electric field $dE/dx$ is $ikE+2E_0$, where $E_0 = E(0)$ is the electric field at the right side $(x > 0)$ of the plasma boundary. Substituting $f_k$ from (B9) into (B10) yields

$$E_k = \frac{2E_0}{ik} \frac{1}{\varepsilon_{||}(\omega, k)} \tag{B11}$$

where $\varepsilon_{||}(\omega, k)$ is the longitudinal plasma permittivity

$$\varepsilon_{||}(\omega, k) = 1 + \frac{\omega_p^2}{n_0 k} \int_{-\infty}^{\infty} \frac{1}{\omega + i\nu - v_x k} \frac{df_0}{dv_x} \, dv_x. \tag{B12}$$

Substituting a Maxwellian EEDF

$$f_0 = \frac{n_0}{\sqrt{\pi} v_T} \exp\left(-v^2 / v_T^2\right) \tag{B13}$$

where $v_T = \sqrt{2T/m}$, into (B12) and after some algebra [3], we obtain

$$\varepsilon_{||}(\omega, k) \simeq 1 + \frac{2\omega_p^2}{k^2 v_T^2} \left[1 + \frac{1}{\sqrt{\pi} v_T} \int_{-\infty}^{\infty} \frac{\exp\left(-v^2 / v_T^2\right)}{v_x k - \omega - i\nu} \, dv_x \right]. \tag{B14}$$

The last term on the right hand side can be expressed in terms of the plasma dispersion function

$$Z(\zeta) = \frac{1}{\sqrt{\pi}} \int_{-\infty}^{\infty} \frac{\exp(-t^2)}{t - \zeta} dt, \quad \mathrm{Im}(\zeta) > 0. \tag{B15}$$

The dispersion function $Z(\zeta)$ in the form of (B15) is only defined for $\mathrm{Im}(\zeta) > 0$ and is defined as an analytical continuation for $\mathrm{Im}(\zeta) < 0$. For $k > 0$, in the limit $\nu \to 0$

$$\frac{1}{\sqrt{\pi} v_T} \int_{-\infty}^{\infty} \frac{\exp\left(-v^2 / v_T^2\right)}{v_x k - \omega - i\nu} dv_x = \frac{1}{kV_T/\omega} Z(\omega / kV_T). \tag{B16}$$

For $k < 0$, the imaginary part of the $(\omega + i\nu)/k$ is negative and we have to transform the integral (B14) so that the pole $v_{xp} = (\omega + i\nu)/k$ lies in the upper plane of the complex velocity. This can be achieved by substitution $-v_x \to v_x$, which gives for $k < 0$

$$\frac{1}{\sqrt{\pi} v_T} \int_{-\infty}^{\infty} \frac{\exp\left(-v^2 / v_T^2\right)}{v_x |k| - \omega - i\nu} dv_x = \frac{1}{|k| v_T / \omega} Z(\omega / |k| v_T). \tag{B17}$$

As a result

$$\varepsilon_{||}(\omega, k) \simeq 1 + \frac{2\omega_p^2}{k^2 v_T^2} \left[1 + \frac{1}{|kV_T/\omega|} Z(|\omega / kV_T|)\right]. \tag{B18}$$

Note that because the function $f_0$ is symmetric with respect to the substitution $-v_x \to v_x$, $\varepsilon(\omega, k)$ is symmetric with respect to the substitution $-k \to k$. Correspondingly, the symmetry of the electric field in (B8) is preserved.

The electric field profile is given by the inverse Fourier transform of (B11)

$$E_x(x) = \frac{1}{2\pi} \int_{-\infty}^{\infty} \frac{2E_0}{ik} \frac{e^{ikx}}{\varepsilon_{||}(\omega, k)} \, dk. \tag{B19}$$

In the limit $x \to \infty$, $E(x) \to E_0/\varepsilon$, where $\varepsilon = \varepsilon(\omega, 0)$. This is in accord with the conservation of the total current in the 1-D geometry. The total current is the sum of the displacement current and the electron current

$$\frac{1}{4\pi} \frac{\partial E_x}{\partial t} + j_e = I(t). \tag{B20}$$

The total current conservation follows from the combination of the Poisson equation and the charge continuity equation. Indeed, taking the time derivative of the Poisson equation and making use of the charge continuity equation gives

$$\nabla \cdot \frac{\partial}{\partial t} E_x + 4\pi \nabla \cdot j_e = 0. \tag{B21}$$

In 1-D geometry it can be integrated with a constant of space—the total current carrying through the plasma $I(t)$, which gives (B20). For a harmonic electric field considered here, (B20) gives

$$-i\omega E_x - 4\pi i\omega \left(\frac{\varepsilon - 1}{4\pi}\right) E_x = -i\omega E_0. \tag{B22}$$

Here, we account for the relationship between the plasma conductivity ($j_e = \sigma E$) and the plasma dielectric function $\varepsilon = 1 + 4\pi\sigma/(-i\omega)$. Equation (B22) gives

$$E_x(x \to \infty) = E_0/\varepsilon. \tag{B23}$$

The same result can be obtained from (B19) after substituting $\varepsilon(\omega,k)\to\varepsilon(\omega,0)$ and integrating. Thus, the electric field in the transition region is given by

$$E_x(x)-E_0/\varepsilon=\frac{1}{2\pi}\int_{-\infty}^{\infty}\frac{2E_0}{ik}\times\left(\frac{1}{\varepsilon_{||}(\omega,k)}-\frac{1}{\varepsilon_{||}(\omega,0)}\right)e^{ikx}\,dk. \quad \text{(B24)}$$

The dielectric function in the form given by (B14) is not an analytic function of $k$. To apply the theory of residues, Landau proposed to split integral into two parts [2] according to

$$E_x(x)-E_0/\varepsilon=\frac{1}{2\pi}\int_{-\infty}^{\infty}\frac{2E_0}{ik}\left(\frac{1}{\varepsilon_1(\omega,k)}-\frac{1}{\varepsilon(\omega,0)}\right)e^{ikx}\,dk+\frac{1}{2\pi}\int_{0}^{\infty}\frac{2E_0}{ik}\left(\frac{1}{\varepsilon_1(\omega,k)}-\frac{1}{\varepsilon_{||}(\omega,k)}\right)e^{ikx}\,dk, \quad \text{(B25)}$$

where

$$\varepsilon_1(\omega,k)=1+\frac{2\omega_p^2}{\omega^2k^2}\left[1-\frac{1}{kv_T/\omega}Z(-\omega/kv_T)\right]. \quad \text{(B26)}$$

The first integral can be calculated by moving the path of integration into the complex $k$ plane and applying the theory of residues. For $\omega\ll\omega_p$, $\varepsilon<0$ and there is only one pole $\varepsilon_1(\omega,k)=0$ in the upper half-plane [2]. It corresponds to the usual screening with the Debye length. In the limit $k\sim\omega_p/v_T$, $Z(|\omega/kv_T|)\sim 1$ and $Z(|\omega/kv_T|)/|kv_T/\omega|\ll 1$, which gives

$$\varepsilon_1(\omega,k)\simeq 1+\frac{2\omega_p^2}{k^2v_T^2}. \quad \text{(B27)}$$

Calculation of the first term in (B26) gives $E_0\exp(-x/a)$, where $a$ is the Debye length $a=v_T/\sqrt{2}\omega_p$. Therefore

$$E_x(x)=E_0/\varepsilon+E_0\exp(-x/a)+\frac{1}{2\pi}\int_{0}^{\infty}\frac{2E_0}{ik}\left(\frac{\varepsilon_{||}(\omega,k)-\varepsilon_1(\omega,k)}{\varepsilon_1(\omega,k)\varepsilon_{||}(\omega,k)}\right)e^{ikx}\,dk. \quad \text{(B28)}$$

For $\mathrm{Im}(k)=0$, $Z(-\omega/kv_T)=-Z(\omega/kv_T)^*$ [4] and

$$\varepsilon_1(\omega,k)=1+\frac{2\omega_p^2}{v_T^2k^2}\left[1+\frac{1}{kv_T/\omega}Z(\omega/kv_T)^*\right]. \quad \text{(B29)}$$

Substituting (B29) into (B28) gives for the last term $E_t(x)$

$$E_t(x)=\frac{4E_0}{\pi}\frac{\omega\omega_p^2}{v_T^3}\int_0^{\infty}\frac{1}{k^4}\frac{\mathrm{Im}[Z(\omega/kv_T)]}{\varepsilon_1(\omega,k)\varepsilon_{||}(\omega,k)}e^{ikx}\,dk, \quad \text{(B30)}$$

where [4]

$$\mathrm{Im}[Z(\zeta)]=\sqrt{\pi}\exp(-\zeta^2). \quad \text{(B31)}$$

The last integral can be calculated analytically only in the limit $x\gg v_T/\omega$ by applying the method of steepest descent. In this limit, $k\ll v_T/\omega$, $\varepsilon_1(\omega,k)\approx\varepsilon(\omega,k)\approx\varepsilon$ and

$$\int_0^{\infty}\frac{1}{k^4}\exp\left(ikx-\omega^2/k^2v_T^2\right)dk\simeq\frac{\sqrt{2\pi}}{\sqrt{3}}(x\lambda_\omega)^{2/3}\lambda_\omega\exp\left[c\left(\frac{x}{\lambda_\omega}\right)^{2/3}-i\pi/3\right] \quad \text{(B32)}$$

where $c=3(-1+i\sqrt{3})/4$, and $\lambda_\omega=v_T/\sqrt{2}\omega$ is the phase-mixing scale.

Substituting (B31) into (B30) and making use of (B32) yields at $x\gg\lambda_\omega$ [2]

$$E_t(x)\approx\frac{2E_0}{\sqrt{3}\varepsilon^2}\frac{\omega_p^2}{\omega^2}\left(\frac{x}{\lambda_\omega}\right)^{2/3}\exp\left[c\left(\frac{x}{\lambda_\omega}\right)^{2/3}-i\pi/3\right]. \quad \text{(B33)}$$

The plots of amplitude and phase of the electric field profile $E_t(x)$ given by (B30) and the approximate analytical result (B33) are shown in Fig. 2.

## Appendix C
## Analytical Derivation of the Transverse RF Electric Field Profile Near the Plasma Boundary ($\mathbf{E}\perp\mathbf{k}$)

The analytical solution involves solving the Vlasov equation for the electron velocity distribution function (EVDF) $F$

$$\frac{\partial F}{\partial t}+v_x\frac{\partial F}{\partial x}-\frac{e}{m}(E_y+v_x\times B_z)\frac{\partial F}{\partial v_y}=0. \quad \text{(C1)}$$

This equation has to be solved together with the Maxwell's equation yielding

$$\left(\frac{d^2}{dx^2}+\frac{\omega^2}{c^2}\right)E_y=-\frac{4\pi i\omega}{c^2}[j+I\delta(x)] \quad \text{(C2)}$$

where $I$ is the surface current. The plasma density is not perturbed in the transverse electric field; therefore there is no need to solve the Poisson equation. In the linear approximation, the EVDF can be split into two parts

$$F(t,x,\mathbf{v})=f_0(v)+f(t,x,\mathbf{v}) \quad \text{(C3)}$$

where $f_0(v)$ describes EVDF of an isotropic, uniform plasma with uniform ion density $n_e=n_i=n_0$ and $f(t,x,\mathbf{v})$ is the EVDF perturbation due a RF electromagnetic field. Substituting (C3) into (C1) yields the linearized Vlasov equation

$$\frac{\partial f}{\partial t}+v_x\frac{\partial f}{\partial x}-\frac{e}{m}E_y\frac{\partial f_0}{\partial v_y}=-\nu f. \quad \text{(C4)}$$

$$E_{yp}(x) = \frac{2\pi i\omega}{c^2} I \int_{-\infty}^{\infty} \frac{e^{ikx}}{k^2 - \omega^2 \varepsilon_{t1}(\omega,k)/c^2} dk \tag{C14}$$

and

$$E_{yt}(x) = \frac{2i\omega}{c^2} I \frac{\omega^2}{c^2} \int_{0}^{\infty} \frac{[\varepsilon_t(\omega,k) - \varepsilon_{t1}(\omega,k)]e^{ikx}}{[k^2 - \omega^2\varepsilon_{t1}(\omega,k)/c^2][k^2 - \omega^2\varepsilon_t(\omega,k)/c^2]} dk \tag{C15}$$

$$\varepsilon_{t1}(\omega,k) = 1 - \frac{\omega_p^2}{\omega^2} \frac{\omega}{v_T k} Z\left(-\frac{\omega}{v_T k}\right) \tag{C16}$$

In (C4), the small collisional term with collision frequency $\nu \ll \omega$ is taken into account. Similarly to the case of the longitudinal electric field, we can consider the entire plane $x \in [-\infty, \infty]$ by artificially continuing the electric field in the semi-plane $x < 0$. The Vlasov equation is symmetric relative to the change in variables according to the substitution

$$v_x \to -v_x, x \to -x, E_y \to E_y. \tag{C5}$$

Therefore, electrons at $x = 0$ with $v_x > 0$ which are reflected from the wall can be represented as electrons which came from the semi-plane $x < 0$ and interacted with the electric field

$$E_y(x < 0) = E_y(x > 0). \tag{C6}$$

As a result, the electric field has to be continued symmetrically into the semi-plane $x < 0$.

Now we can apply the Fourier transform for (C4) and (C2). This gives for components of the EVDF $f_k e^{-i\omega t + ikx}$ and the electric field $E_{yk} e^{-i\omega t + ikx}$

$$-i(\omega + i\nu - v_x k) f_k - \frac{e}{m} E_{yk} \frac{\partial f_0}{\partial v_y} = 0 \tag{C7}$$

$$\left(-k^2 + \frac{\omega^2}{c^2}\right) E_{yk} = -\frac{4\pi i\omega}{c^2}(j_k + I). \tag{C8}$$

Substituting $f_k$ from (C7) into (C8) with the current $j_k = -e\int f_k v_y d\mathbf{v}$ yields

$$E_{yk} = \frac{4\pi i\omega}{c^2} I \frac{1}{k^2 - \frac{\omega^2}{c^2}\varepsilon_t(\omega,k)} \tag{C9}$$

where $\varepsilon_t(\omega,k)$ is the transverse plasma permittivity

$$\varepsilon_t(\omega,k) = 1 + \frac{\omega_p^2}{n_0\omega} \int_{-\infty}^{\infty} \frac{v_y}{\omega + i\nu - v_x k} \frac{\partial f_0}{\partial v_y} dv_x. \tag{C10}$$

Substituting a Maxwellian EEDF gives [3]

$$\varepsilon_t(\omega,k) = 1 + \frac{\omega_p^2}{\omega^2} \frac{\omega}{v_T|k|} Z\left(\frac{\omega}{v_T|k|}\right). \tag{C11}$$

Note that because the function $f_0$ is symmetric relative to the substitution $-v_x \to v_x$, $\varepsilon(\omega,k)$ is symmetric relative to the substitution $-k \to k$. Correspondingly, the symmetry of the electric field in (C9) is preserved.

The electric field profile is given by the inverse Fourier transform of (C9)

$$E_y(x) = \frac{1}{2\pi} \int_{-\infty}^{\infty} \frac{4\pi i\omega}{c^2} I \frac{e^{ikx}}{k^2 - \omega^2\varepsilon_t(\omega,k)/c^2} dk. \tag{C12}$$

Similar to the analysis of the longitudinal electric field, we split the integral in (C9) into two parts

$$E_y(x) = E_{yp}(x) + E_{yt}(x) \tag{C13}$$

where we have (C14)–(C16), found at the top of the page. Note that $\varepsilon_{t1}(\omega,k) = \varepsilon_t(\omega,k)$ for $k < 0$.

The first part $E_{yp}(x)$ of the electric field can be calculated by evaluating the integral in the complex $k$ plane. A pole of $E_{yp}(x) - k_p i$ lies on the imaginary axis of the $k$ plane. The dielectric permittivity is real and negative on imaginary axis of the $k$ plane

$$\varepsilon_{t1}(\omega, k_p i) = 1 - \frac{\omega_p^2}{\omega^2} \frac{\omega}{v_T k_p} F\left(\frac{\omega}{v_T k_p}\right) \tag{C17}$$

where $F(\zeta) = \mathrm{Im}Z(i\zeta) = \sqrt{\pi}\exp(y^2)\mathrm{erfc}(y)$ [4]. There is always a real value of $k_p$ as the root of

$$k_p^2 = -\omega^2\varepsilon_{t1}(\omega, ik_p)/c^2. \tag{C18}$$

Applying the theory of residues, the integral for $E_{yp}(x)$ gives

$$E_{yp}(x) = E_{op} e^{-k_p x} \tag{C19}$$

where

$$E_{op} = \frac{2i\omega}{c^2} \frac{2\pi i I}{2k_p i - d\varepsilon_{t1}(\omega,k)/dk\omega^2/c^2}. \tag{C20}$$

In the limit $x \gg \delta$, the last term $E_{yt}(x)$ can be calculated making use of the method of steepest descent. Substituting $k^2 - \omega^2\varepsilon_{t1}(\omega,k)/c^2$ in the denominator of the expression for $E_{yt}(x)$ by its limit $= \omega_p^2/c^2$ at $k \to 0$, gives

$$E_{yt}(x) = -\frac{4\omega^2\sqrt{\pi}}{\omega_p^2 v_T} I \left[\int_0^{\infty} \frac{1}{k} \exp\left[-\left(\frac{\omega}{v_T k}\right)^2 + ikx\right] dk\right] \tag{C21}$$

which yields

$$E_{ystd}(x) = -\frac{4\omega^2\pi}{\omega_p^2 v_T} I \frac{\sqrt{2}}{\sqrt{3}} \left(\frac{x}{\lambda_\omega}\right)^{-1/3} \times \exp\left[c\left(\frac{x}{\lambda_\omega}\right)^{2/3} - i\pi/2\right] \quad \text{(C22)}$$

where $c = 3(-1+i\sqrt{3})/4$ and $\lambda_\omega = v_T/\sqrt{2}\omega$.

## ACKNOWLEDGMENT

The authors gratefully acknowledge helpful discussions with R. C. Davidson, V. Godyak, E. Kawamura, A. J. Lichtenberg, M. A. Lieberman, B. N. Ramamurthi, E. A. Startsev, M. M. Turner, and L. D. Tsendin.

## REFERENCES

[1] L. Brillouin, Wave Propagation and Group Velocity. New York, Academic, 1960.
[2] L. D. Landau, "On the vibrations of the electronic plasma," in *J. Phys. (USSR)*, 1946, vol. 10, p. 25.
[3] E. M. Lifshitz and L. P. Pitaevskii, Physical Kinetics Pergamon. Oxford, U.K., p. 368, 1981.
[4] J. D. Huba, NRL Plasma Formulary The Office of Naval Research. Arlington,, VA, p. 30, 1994.
[5] V. A. Godyak, "Statistical heating of electrons at an oscillating plasma boundary," *Sov. Phys.-Techn. Phys.*, vol. 16, p. 1073, 1972.
[6] V. Godyak, "Steady-state low-pressure RF discharge," *Sov. J. Plasma Phys.*, vol. 2, p. 78, 1976.
[7] M. A. Lieberman, "Analytical solution for capacitive RF sheath," *IEEE Trans. Plasma Sci.*, vol. 16, no. 6, p. 638, Dec. 1988.
[8] M. A. Lieberman and V. A. Godyak, "From Fermi acceleration to collisionless discharge heating," *IEEE Trans. Plasma Sci.*, vol. 26, no. 3, pp. 955–986, Jun. 1998.
[9] I. D. Kaganovich and L. D. Tsendin, "The space-time-averaging procedure and modeling of the RF discharge II. Model of collisional low-pressure RF discharge," *IEEE Trans. Plasma Sci.*, vol. 20, no. 2, pp. 66–75, Apr. 1992.
[10] I. D. Kaganovich and L. D. Tsendin, "Low-pressure RF discharge in the free-flight regime," *IEEE Trans. Plasma Sci.*, vol. 20, no. 2, pp. 86–92, Apr. 1992.
[11] Yu. M. Aliev, I. D. Kaganovich, and H. Schluter, "Quasilinear theory of collisionless electron heating in radio frequency gas discharges," *Phys. Plasmas*, vol. 4, p. 2413, 1997.
[12] T. J. Sommerer, W. N. G. Hitchon, and J. E. Lawler, "Electron heating mechanisms in helium RF glow discharges: A self-consistent kinetic calculation," *Phys. Rev. Lett.*, vol. 66, p. 2361, 1989.
[13] M. Surendra and D. B. Graves, "Electron acoustic waves in capacity coupled, low-pressure RF glow discharges," *Phys. Rev. Lett.*, vol. 66, p. 1469, 1991.
[14] I. D. Kaganovich, "Anomalous capacitive sheath with deep radio-frequency electric-field penetration," *Phys. Rev. Lett.*, vol. 89, p. 265006, 2002.
[15] G. Gozadinos, M. M. Turner, and D. Vender, "Collisionless electron heating by capacitive RF sheaths," in *Phys. Rev. Lett.*, 2001, vol. 87, p. 135004.
[16] G. W. Hammett and F. W. Perkins, "Fluid moment models for Landau damping with application to the ion-temperature-gradient instability," *Phys. Rev. Lett.*, vol. 64, p. 3019, 1990.
[17] E. Furkal, A. Smolyakov, and A. Hirose, "Nonlocal electron kinetics in a weakly ionized plasma," *Phys. Rev. E*, vol. 58, p. 965, 1998.
[18] F. Brunel, "Not-so-resonant, resonant absorption," *Phys. Rev. Lett.*, vol. 59, p. 52, 1987.
[19] T.-Y. B. Yang, W. L. Kruer, A. B. Langdon, and T. W. Johnston, "Mechanisms for collisionless absorption of light waves obliquely incident on overdense plasmas with steep density gradients," *Phys. Plasmas*, vol. 3, p. 2702, 1996.
[20] K. E. Orlov and A. S. Smirnov, "Calculation of discharge parameters in low-pressure diode-type radio frequency noble gas plasmas," *Plasma Sources Sci. Technol.*, vol. 8, p. 37, 1999.
[21] I. D. Kaganovich, "Effects of collisions and particle trapping on collisionless heating," *Phys. Rev. Lett.*, vol. 82, p. 327, 1999.
[22] U. Buddemeier and I. Kaganovich, "Collisionless electron heating in RF gas discharges. II. Role of collisions and non-linear effects," in *Electron Kinetics and Applications of Glow Discharges*, ser. NATO ASI Series B, Physics, U. Korsthagen and L. Tsendin, Eds. New York: Plenum, 1998, vol. 367, p. 283.
[23] Y. P. Raizer, M. N. Shneider, and N. A. Yatsenko, *Radio-Frequency Capacitive Discharges*. Boca Raton, FL: CRC, 1995.
[24] A. E. Wendt and W. N. G. Hitchon, "Electrons with velocity less than $V_{\rm sh0}$ may experience multiple collisions with the oscillating barrier," *J. Appl. Phys.*, vol. 71, p. 4718, 1992.
[25] A. E. Harrison and A. Elliot, *Klystron Tubes.*, 1st ed. New York: McGraw-Hill, 1947.
[26] R. L. Mace, G. Amery, and M. A. Hellberg, "The electron-acoustic mode in a plasma with hot suprathermal and cool Maxwellian electrons," *Phys. Plasmas*, vol. 6, p. 44, 1999.
[27] V. A. Godyak and R. B. Piejak, "Abnormally low electron energy and heating-mode transition in a low-pressure argon RF discharge at 13.56 MHz," *Phys. Rev. Lett.*, vol. 65, p. 996, 1990.
[28] S. V. Berezhnoi, I. D. Kaganovich, and L. D. Tsendin, "Generation of cold electrons in a low-pressure RF capacitive discharge as an analogue of a thermal explosion," *Plasma Phys. Rep.*, vol. 24, p. 556, 1998.
[29] S. V. Berezhnoi, I. D. Kaganovich, and L. D. Tsendin, "Fast modelling of low-pressure radio-frequency collisional capacitively coupled discharge and investigation of the formation of a non-Maxwellian electron distribution function," *Plasma Sources Sci. Technol.*, vol. 7, p. 268, 1998.
[30] M. A. Lieberman and A. J. Lichtenberg, Principles of Plasma Dischargesand Material Processing2nd ed. Hoboken, NJ, Wiley, p. 401, 2005.
[31] I. D. Kaganovich and L. D. Tsendin, "Collisionless electrode sheath in an RF discharge," *Sov.-Phys. Tech. Phys. Lett.*, vol. 16, p. 43, 1990.
[32] R.-P. Brinkmann, private communication 2005.
[33] Z. Wang, A. J. Lichtenberg, and R. H. Cohen, "Kinetic theory of stochastically heated RF capacitive discharges," *IEEE Trans. Plasma Sci.*, vol. 26, no. 1, pp. 59–68, Feb. 1998.
[34] E. Kawamura, Private Communication 2005.
[35] A. B. Pippard, "The surface impedance of superconductors and normal metals at high frequencies. II. The anomalous skin effect in normal metals," in *Proc. R. Soc. A*, 1947, vol. 191, p. 385.
[36] E. S. Weibel, "Anomalous skin effect in a plasma," *Phys. Fluids*, vol. 10, p. 741, 1967.
[37] V. I. Kolobov and D. J. Economou, "The anomalous skin effect in gas discharge plasmas," *Plasma Sources Sci. Technol.*, vol. 6, p. R1, 1997.
[38] I. D. Kaganovich and O. Polomarov, "Self-consistent system of equations for a kinetic description of the low-pressure discharges accounting for the nonlocal and collisionless electron dynamics," *Phys. Rev. E*, vol. 68, p. 026411, 2003.
[39] V. A. Godyak, R. B. Piejak, and B. M. Alexandrovich, "Electron energy distribution function measurements and plasma parameters in inductively coupled argon plasma," *Plasma Sources Sci. Technol.*, vol. 11, p. 525, 2002.
[40] A. N. Kondratenko, *Field Penetration into a Plasma* (in Russian). Moscow, USSR: Nauka, 1979, p. 30.
[41] A. F. Alexandrov, L. S. Bogdankevich, and A. A. Rukhazde, Principles of Plasma Electrodynamics. Berlin, Germany, Springer-Verlag, p. 344, 1984.
[42] V. A. Godyak, "Plasma phenomena in inductive discharges," *Plasma Phys. Control. Fusion*, vol. 45, p. A339, 2003.
[43] V. Vahedi, M. A. Lieberman, G. DiPeso, T. D. Rognlien, and D. Hewett, "Analytic model of power deposition in inductively coupled plasma sources," *J. Appl. Phys.*, vol. 78, p. 1446, 1995.
[44] F. A. Haas, "Some aspects of collisionless heating in inductive discharges," *Plasma Sources Sci. Technol.*, vol. 10, p. 440, 2001.
[45] Yu. O. Tyshetskiy, A. I. Smolyakov, and V. A. Godyak, "Reduction of electron heating in the low-frequency anomalous-skin-effect regime," *Phys. Rev. Lett.*, vol. 90, p. 255002, 2003.
[46] O. Polomarov, C. E. Theodosiou, and I. D. Kaganovich, "Enhanced collisionless heating in a nonuniform plasma at the bounce resonance condition," *Phys. Plasmas*, vol. 12, p. 80704, 2005.
[47] I. D. Kaganovich, E. A. Startsev, and G. Shvets, "Anomalous skin effect for anisotropic electron velocity distribution function," *Phys. Plasmas*, vol. 11, p. 3328, 2004.
[48] B. Ramamurthi, D. J. Economou, and I. D. Kaganovich, "Effect of nonlocal electron conductivity on power absorption and plasma density profiles in low pressure inductively coupled discharges," *Plasma Sources Sci. Technol.*, vol. 12, p. 170, 2003.

[49] B. Ramamurthi, D. J. Economou, and I. D. Kaganovich, "Effect of electron energy distribution function on power deposition and plasma density in an inductively coupled discharge at very low pressures," *Plasma Sources Sci. Technol.*, vol. 12, p. 302, 2003.

[50] I. D. Kaganovich, O. V. Polomarov, and C. E. Theodosiou, "Landau damping and anomalous skin effect in low-pressure gas discharges: Self-consistent treatment of collisionless heating," *Phys. Plasmas*, vol. 11, p. 2399, 2004.

[51] O. Polomarov, C. E. Theodosiou, and I. D. Kaganovich, "Self-consistent modeling of nonlocal inductively coupled plasmas," *Abstract 31st. IEEE Int. Conf. Plasma Sci. 2004*, p. 230, Jun.–Jul. 2005.

[52] Yu. M. Aliev, I. D. Kaganovich, and H. Schluter, Collisionless Electron Heating in RF Gas Discharges. I. Quasilinear Theory ser. NATO ASI Series B, Physics, U. Korsthagen and L. Tsendin, Eds. New York, , Plenum, vol. 367, p. 257, 1998.

[53] Yu. O. Tyshetskiy, "Anomalous and nonlinear effects in inductively coupled plasmas," Ph.D. dissertation, University of Saskatchewan, Saskatoon,, SK, Canada, 2003 [Online]. Available: http://library.usask.ca/theses/available/etd-12182003-161103

**Igor D. Kaganovich** received the B.S. and M.S. degrees from the Physical–Mechanical Department, St. Petersburg Technical University, St. Petersburg, Russia, and the Ph.D. degree from Ioffe Physical Technical Institute, St. Petersburg, Russia.

He is the Research Physicist at Princeton Plasma Physics Laboratory (PPPL), Princeton, NJ. His professional interests include plasma physics with applications to nuclear fusion (heavy ion fusion), gas discharge modeling, and plasma processing, kinetic theory of plasmas and gases, hydrodynamics, quantum mechanics, nonlinear phenomena, and pattern formation.

Dr. Kaganovich was the recipient of the Alexander von Humboldt Fellowship in 1996. His research was supported by individual grants from international and national funding agencies including DOE, NSF, INTAS, ISF, and RFBR.

**Oleg V. Polomarov** received the diploma and the M.S. degree in theoretical physics from the Kiev State University, Kiev, Ukraine, in 1992 and the Ph.D. degree in plasma physics from the University of Toledo, Toledo, OH, in 2005.

He is presently a postdoctoral fellow at the Institute for Fusion Studies, University of Texas, Austin, Austin. His primary research interests are kinetic aspects of discharge modeling, nonlinear dynamics, and resonant excitation of strong plasma waves.

**Constantine E. Theodosiou** received the diploma from the University of Athens, Athens, Greece, in 1977 and the M.S. and Ph.D. degrees from the University of Chicago, Chicago, IL, all in physics.

Following a two-year postdoctoral at Johns Hopkins University, Baltimore, MD, he spent two years at the University of Freiburg, Freiburg, Germany, as an Alexander von Humboldt Fellow. After a year as a Visiting Faculty Member at Drexel University, Philadelphia, PA, he joined in 1981, the Physics and Astronomy Department at the University of Toledo, Toledo, OH, where he is currently Professor of Physics and Associate Dean for the Natural Sciences and Mathematics. His primary research interests include calculations of atomic structure, atomic collisions, photon–atom interactions, and computer simulations of gas discharges, e.g., in plasma display panels.